




# A review on recent advances in carbon-based dielectric system for microwave absorption

Liru Cui<sup>1</sup>, Xijiang Han<sup>1,\*</sup>, Fengyuan Wang<sup>1</sup>, Honghong Zhao<sup>1</sup>, and Yunchen Du<sup>1,\*</sup> 

<sup>1</sup> MIIT Key Laboratory of Critical Materials Technology for New Energy Conversion and Storage, School of Chemistry and Chemical Engineering, Harbin Institute of Technology, Harbin 150001, China

**Received:** 27 November 2020

**Accepted:** 15 February 2021

**Published online:**  
3 March 2021

© The Author(s), under exclusive licence to Springer Science+Business Media, LLC part of Springer Nature 2021

## ABSTRACT

Microwave absorbing materials (MAMs), which have been highly developed in the past two decades, are being regarded as a kind of functional materials to combat electromagnetic (EM) pollution, because they can provide sustainable energy conversion rather than simple reflection of incident EM waves. Although traditional magnetic materials can dissipate EM energy effectively, they always suffer from some intrinsic drawbacks, such as high density, easy corrosion, and skin effect, which make them unpopular in many practical applications. Therefore, the rational design of pure dielectric system without any magnetic components is becoming a new frontier topic for MAMs. Among various candidates, carbon-based dielectric system almost dominates the development of non-magnetic MAMs. This review presents a comprehensive introduction on the recent advances of carbon-based dielectric system composed of carbon materials and other dielectric components, including metal oxides/carbon, metal sulfides/carbon, conductive polymers/carbon, carbides/carbon, carbon/carbon, and various ternary carbon-based dielectric composites. Thanks to the synergistic effects between different components and the elaborate microstructure design, these carbon-based dielectric composites can produce superior microwave absorption performance to traditional magnetic materials. Moreover, the challenges and prospects are also proposed to indicate some new insights for the further research of carbon-based dielectric system.

Handling Editor: Joshua Tong.

Address correspondence to E-mail: hanxijiang@hit.edu.cn; yunchendu@hit.edu.cn

## Introduction

Since Maxwell published his great paper ‘A dynamical theory of the electromagnetic field’ in 1865, the heart of twentieth and twenty-first century physics, as elaborated by Einstein and others, electromagnetic (EM) theory has rapidly evolved into one of the most important sources of science and technology for human beings, which motivated us to make continuous breakthroughs in the field of wireless communication [1]. Especially with the advent of 5G era, there will be drastically increasing numbers of electronic devices in all aspects of people’s life. However, while enjoying the convenience of life, we must pay attention to the accompanied EM pollution, because it may pose considerable threats to EM interference, information security, and public health [2, 3]. To date, there are two popular strategies used for the precaution of EM pollution, i.e. shielding and absorption [4, 5]. Compared with traditional shielding strategy established on reflection principle, microwave absorption is receiving more and more attention for its tackling these adverse effects through sustainable conversion of EM energy [6, 7]. Microwave absorbing materials (MAMs), as the core component of this advanced pathway, are expected to make a solid contribution to progressively serious EM pollution [8–10].

In the past decades, magnetic materials, including magnetic metals and ferrites, have been extensively studied as powerful MAMs as they could block the transmission of EM waves by interacting with the magnetic branches, and in many cases, magnetic metals could even provide compatible dielectric loss mechanism [11, 12]. It is unfortunate that some intrinsic drawbacks, such as easy corrosion, low Curie temperature, and high density, make them undesirable for practical applications [13, 14]. In view of these shortcomings, different strategies have been adopted to modify magnetic materials, such as magnetic anisotropy adjustment, surface coating, microstructure design, and so on [15–17]. Although some achievements have been achieved in the implementation of those modification strategies, corrosion or oxidation of magnetic particles is still inevitable. What’s worse, the introduction of non-magnetic components may weaken the interaction between magnetic particles, resulting in a significant decrease in magnetic loss [18]. As a result, some

groups attempted to develop absolute dielectric loss system that is free of any magnetic components, and a lot of successful examples demonstrated that a single dielectric system may not only produce comparable microwave absorption performance to conventional magnetic materials, but also untangle some intrinsic drawbacks of magnetic materials [19, 20]. Such a situation renders absolute dielectric loss system as a kind of promising candidates that may cater to the high demands for the next generation of MAMs, i.e. lightweight, thin thickness, strong absorption, and wide-frequency response [21, 22]. Among various dielectric loss media, carbon materials always reside at the frontier of high-performance MAMs due to their unique advantages in low density, chemical stability, tailorable dielectric property, good processability, and diverse forms [23–25]. In an effort to reinforce microwave absorption performance of carbon materials, many secondary dielectric components are purposefully introduced to enrich loss mechanisms, improve impedance matching, and broaden response bandwidth [26, 27].

It is widely accepted that an EM functionalized medium can dissipate EM energy through magnetic loss and dielectric loss [28–30]. However, magnetic components are always excluded in absolute carbon-based dielectric system, and thus dielectric loss will be the only mechanism for its microwave absorption. According to the classical dielectric theory, dielectric loss is mainly determined by conductivity loss and polarization loss [31, 32]. High conductivity greatly favors strong conductivity loss, because this loss process originates from the heat effect of micro-current induced by residual carriers in dielectric medium [33]. In contrast, polarization loss is relatively complicated, which can be further classified as ionic polarization, electronic polarization, dipole orientation polarization, and interfacial polarization [34]. By considering that ionic polarization and electronic polarization are elastic and too fast ( $10^{-15} \sim 10^{-12} \text{ s}^{-1}$ ), they will not have considerable contribution to microwave absorption, and thus dipole orientation polarization and interfacial polarization are two effective modes for microwave absorption [35]. Some bound charges at the defective sites and residual groups can act as the dipoles of dielectric medium, and the energy consumption may be triggered when they reorient themselves along with the direction of an applied EM field [36]. As for interfacial polarization, it comes from the uneven

accumulation and distribution of space charges at the interfaces, and these numerous microcosmic electric moments will also produce considerable energy dissipation [37, 38]. The overall dielectric loss capability of absolute carbon-based dielectric system from conductivity loss, dipole orientation polarization, and interfacial polarization can be depicted by dielectric dissipation factor ( $\tan\delta_e = \varepsilon_r''/\varepsilon_r'$ ). Of note is that the blind pursuit of a dielectric dissipation factor cannot bring good microwave absorption performance, especially in the absence of magnetic components, because there is another important factor, impedance matching, to determine microwave absorption [39]. If the characteristic impedance of dielectric medium is mismatched with that of free space, there will be strong reflection of incident EM waves at the front interface, and microwave absorption will be poor no matter how powerful its intrinsic loss capability [40]. Only in the case of matched impedance can incident EM waves be attenuated effectively [41]. Therefore, all existing references about absolute carbon-based dielectric system are devoted to powerful dielectric loss capability and good impedance matching simultaneously.

Although many high-performance MAMs have been summarized and discussed in some important reviews [42, 43], a systematic introduction of various carbon-based dielectric composites is rarely reported. With more and more publications in the related field, a comprehensive review of the research results will be greatly helpful to further accelerate the development of carbon-based dielectric system for microwave absorption. In this context, we highlight some recent advances of non-magnetic carbon-based composites as high-performance MAMs, including metal oxides/carbon, metal sulfides/carbon, conductive polymers/carbon, carbides/carbon, carbon/carbon, and ternary carbon-based dielectric composites, and we also propose some disadvantages, challenges, and prospects in this field.

### Metal oxides/carbon composites

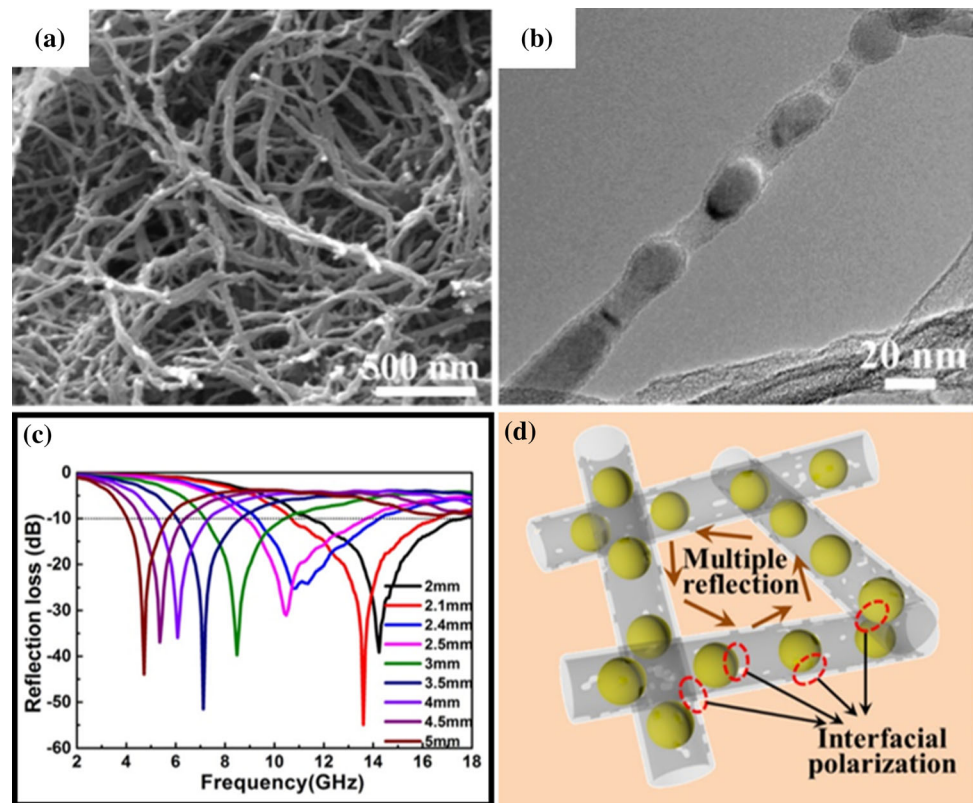
Metal oxides are a kind of solid materials that are composed of oxygen element and one or more metal elements, and some intrinsic features make them potentially effective in microwave absorption. First, thanks to the nature of ionic metal–oxygen bonding, there will be desirable polarization effect in metal

oxides under an applied EM field, driving the transformation from ionic crystals to metallic/covalent crystals [44–46]. Second, the existence of multivalence states in some P-zone metal elements and transition metal elements may generate non-metrological defect sites, which can also play as dipoles to consume the energy of an applied EM field [47–49]. Third, the electronic transitions in some semiconductors are further helpful to provide auxiliary conductive loss through the formation of micro current [50–52]. In the past decades, some groups paid much attention to morphology design, defect creation, and crystal phase optimization to consolidate the microwave absorption performance of metal oxides [53–55]. Although some improvements have been achieved through these strategies, a gap to practical application still exists due to their ordinary polarization loss and conductive loss.

The combination of metal oxides and carbon materials has been demonstrated as an effective way to make up their drawbacks [56]. On one hand, carbon materials can increase the overall dielectric loss capability of these composites through enhanced conductive loss and dipole orientation polarization [57], and on the other hand, metal oxides can remedy their characteristic impedance to suppress strong reflection of EM waves at the incident surface of MAMs [58]. What's more, such a combination also brings sufficient heterogeneous interfaces between metal oxides and carbon materials and results in an additional loss mechanism, i.e. interfacial polarization, from the uneven space charges at these interfaces [59]. Therefore, high dispersion of metal oxides nanoparticles on the surface of carbon materials is becoming an important topic in determining the microwave absorption performance of the related composites [60]. Wu et al. tailored the size of MoO<sub>2</sub> clusters on reduced graphene oxide (RGO) through a supermolecular-scale cage-confinement route, and they confirmed uniform dispersion of MoO<sub>2</sub> clusters made a solid contribution to microwave absorption. The minimum reflection loss (RL) value of the resultant composite could reach –35.4 dB at 16.0 GHz with just 1.5 mm thickness, which is better than many RGO-based composites, even those loaded with magnetic nanoparticles [61].

As we mentioned above, carbon materials have diversified morphology and microstructure, and thus rational design on the morphology and microstructure is also a hot topic in metal oxides/carbon

**Figure 1** SEM image (a), TEM image (b), RL curves (c), and possible microwave absorption mechanisms (d) of peapod-like MnO@CNWs. Adapted from Ref. [62], Copyright: 2018 American Chemical Society. Used with permission.



composites. As shown in Fig. 1, Duan et al. investigated EM properties of peapod-like MnO@carbon nanowires (MnO@CNWs), and they found that the enhanced microwave absorption benefited from dielectric polarization in conductive networks composed of MnO nanoparticles and CNWs, as well as multiple reflection and absorption behaviors of incident EM waves induced by internal void space among CNWs [62]. Our group previously fabricated core-shell BaTiO<sub>3</sub>@carbon microspheres with a space-confined strategy, and a series of comparative experiments clearly witnessed that core-shell microstructure could be taken as a desirable configuration for microwave absorption, where the minimum RL value can reach up to  $-88.5$  dB at 6.9 GHz with the thickness of 3.0 mm [63]. It is very interesting that these core-shell BaTiO<sub>3</sub>@carbon microspheres not only exhibit comparable RL characteristics with common magnetic MAMs, but also address their unique superiority in corrosion resistance. Along with the flourish of nanotechnology, three-dimensional carbon frameworks are emerging as a kind of promising scaffolds for metal oxides/carbon composites, because they can intensify multiple reflection behaviors of incident EM waves

therein, and meanwhile, their extremely high porosity is very favorable for the lightweight of MAMs. When TiO<sub>2</sub> nanoparticles are loaded in three-dimensional carbon nanotubes (3D CNTs) sponge, the resultant TiO<sub>2</sub>/CNTs sponge will harvest powerful RL and achieve equivalent response bandwidth with less absorber thickness [64]. Similar phenomena have also been observed in various 3D carbon-based composites with ZnO, MnO, and CeO<sub>2</sub> nanoparticles [65–67].

It has to mention that some studies realize the enhancement of EM functions through elaborate optimization on metal oxides in these composites. Apart from the loading content of metal oxides in carbon substrates, crystallinity is proved to be a key factor for EM properties of these composites. For example, when amorphous SnO<sub>2</sub> nanoparticles deposited on the surface of carbon fibers (CFs) are completely transformed into rutile phase, the relative complex permittivity and dielectric loss tangent of SnO<sub>2</sub>/CFs composite will be increased visibly [68]. As a result, the effective absorption bandwidth (EAB), which is usually defined as the frequency bandwidth with RL intensity less than  $-10.0$  dB, is broadened from 5.1 GHz (12.9–18.0 GHz) to



15.0 GHz (3.0–18.0 GHz) by integrating the absorber thickness from 1.3 to 5.5 mm, and the optimal matching thickness is drastically reduced from 4.9 to 1.3 mm. Besides, the morphology of metal oxides can also affect the EM properties of their carbon-based composites. Wang et al. compared the microwave absorption performance of graphene-based composites containing NiO, a common anti-ferromagnetic medium, with different morphologies, and the results witnessed that porous flower-like NiO coupled with graphene could display more powerful RL (minimum RL of  $-59.6$  dB) than the counterparts with stratiform-like (minimum RL of  $-8.7$  dB) and particle-like NiO (minimum RL of  $-9.5$  dB) [69]. The enhancement mechanism is similar to that of 3D carbon frameworks discussed above. Although the construction of 3D flower-like morphology in metal oxides is not as easy as that in carbon materials, there are still some successful examples on  $\text{MnO}_2$  and  $\text{BiFeO}_3$  that have been reported in carbon-based MAMs [70–72]. More recently, some researchers further proposed to reinforce the microwave absorption performance of metal oxides/carbon composites by creating abundant oxygen vacancies [73]. Especially for  $\text{ABO}_3$  type perovskite oxides, if A-site cation is missing, oxygen vacancies and highly oxidative O and B sites will appear in  $\text{ABO}_3$ , which will strengthen the polarization relaxation process of B-O dipoles [74]. Following this idea, Jia et al. ever designed  $\text{La}_x\text{FeO}_{3-y}$  with different oxygen vacancies and fabricated a series of  $\text{La}_x\text{FeO}_{3-y}/\text{RGO}$  composites, and they confirmed that the dielectric loss of these composites was highly dependent on the content of oxygen vacancy [75]. This is because the strong electrostatic interaction between the highly

oxidative  $\text{Fe}^{4+}$  in  $\text{La}_x\text{FeO}_{3-y}$  and the negatively charged functional groups in RGO is beneficial to structural stability and interfacial polarization (Fig. 2a), and the defects in RGO and  $\text{La}_x\text{FeO}_{3-y}$  are together responsible for the strengthening of dipole orientation polarization (Fig. 2b). Table 1 summarizes the minimum RL intensities and EABs of various metal oxides/carbon composites in recent studies, where EABs are measured with the absorber thickness of 2.0 mm (a common value for RL evaluation). One can see that most composites can display strong RL intensity, while their EABs are usually located in high frequency range and less than 4.0 GHz, which imply that low-frequency RL and broad EAB are still the main challenges for this kind of MAMs.

### Metal sulfides/carbon composites

Compared with metal oxides, transition metal sulfides usually have narrower band gaps, which means that the transition of electrons from valence band to conduction band will be relatively easy, and thus they can provide stronger conductivity loss capability than conventional metal oxides [76–78]. This intrinsic advantage drives the development of transition metal sulfides/carbon composites in the field of microwave absorption. However, the synergistic effects between transition metal sulfides and carbon materials still need to be carefully controlled. Lu et al. tailored the amount of CdS nanoparticles attached on multi-walled CNTs (MWCNTs), and they found that highly dispersed CdS nanoparticles could promote microwave absorption performance greatly arising from the effective impedance matching, as well as proper dielectric loss [79]. Once CdS nanoparticles were

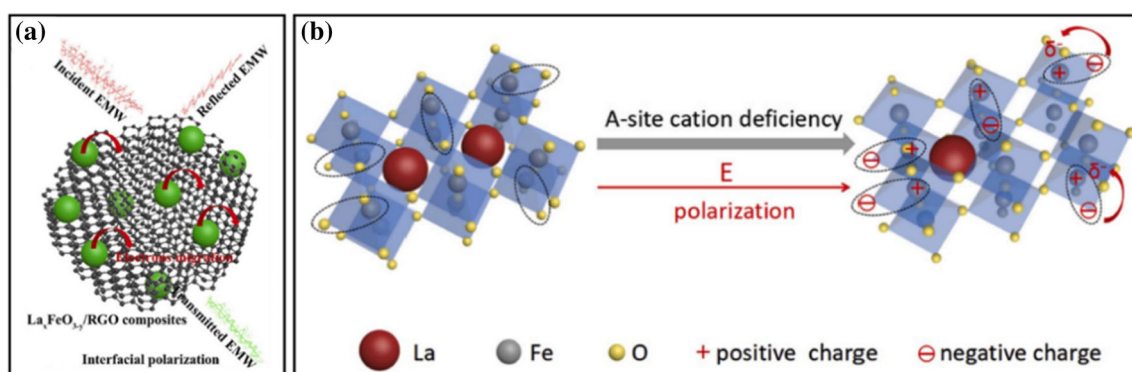


**Figure 2** Schematic illustration of interfacial polarization (a) and dipole orientation polarization (b) of  $\text{La}_x\text{FeO}_{3-y}$ . Adapted from Ref. [75], Copyright: 2020 Elsevier. Used with permission.

**Table 1** Microwave absorption performance of metal oxides/carbon composites

Absorber	Minimum RL (frequency, thickness)	EAB at 2.0 mm (range)	Reference
ZnO/RGO	– 55.7 dB (14.8 GHz, 2.0 mm)	5.0 GHz (12.5–17.5 GHz)	[56]
ZrO <sub>2</sub> /C	– 58.7 dB (16.8 GHz, 1.5 mm)	3.3 GHz (10.2–13.5 GHz)	[58]
MnO/C	– 51.6 dB (10.4 GHz, 2.5 mm)	3.0 GHz (11.1–14.1 GHz)	[60]
MnO@CNWs	– 55.0 dB (13.6 GHz, 2.1 mm)	6.2 GHz (11.4–17.6 GHz)	[62]
BaTiO <sub>3</sub> @C	– 88.5 dB (6.9 GHz, 3.0 mm)	3.0 GHz (9.0–12.0 GHz)	[63]
CNT@TiO <sub>2</sub>	– 31.8 dB (10.4 GHz, 2.0 mm)	2.8 GHz (9.2–12.0 GHz)	[64]
3D graphene/ZnO	– 48.1 dB (11.7 GHz, 1.8 mm)	2.6 GHz (9.5–12.1 GHz)	[65]
C/MnO	– 58.5 dB (13.2 GHz, 1.7 mm)	2.0 GHz (10.0–12.0 GHz)	[66]
MWCNTs/CeO <sub>2</sub>	– 51.1 dB (8.9 GHz, 2.6 mm)	2.6 GHz (11.2–13.8 GHz)	[67]
CFs@SnO <sub>2</sub>	– 44.9 dB (15.8 GHz, 1.3 mm)	Unshown	[68]
NiO@graphene	– 59.6 dB (14.2 GHz, 1.7 mm)	3.8 GHz (10.4–14.2 GHz)	[69]
MnO <sub>2</sub> /RGO	– 37.1 dB (10.8 GHz, 2.0 mm)	4.1 GHz (8.6–12.7 GHz)	[70]
RGO/CeO <sub>2</sub>	– 49.2 dB (5.2 GHz, 4.5 mm)	2.9 GHz (11.3–14.2 GHz)	[73]
La <sub>x</sub> FeO <sub>3-y</sub> /RGO	– 36.2 dB (13.6 GHz, 2.0 mm)	3.9 GHz (11.7–15.6 GHz)	[75]

connected to form a dense sheath, even less than 10 nm, the electron transfer in the conductive carbon networks would be drastically weakened, finally resulting in the degradation of microwave absorption. Similar conclusion can also be indexed in SnS nanosheets/GO and CoS nanoplates/MWCNTs composites [76, 80]. Another advantage of transition metal sulfides is from various self-assembly hierarchical microstructures [81, 82]. In many cases, the self-assembly process may be directed by the surface functional groups of carbon materials, which not only inhibits the aggregation of individual components, but also effectively increases EM loss capability. For example, Chen et al. fabricated  $\alpha$ -MnS hollow spheres/RGO (MHSs-RGO) hybrids by a one-pot template-free solvothermal method [83]. A series of comparative tests showed that a suitable dosage of RGO might contribute to the nucleation and growth of  $\alpha$ -MnS, owing to the interaction of oxygen-containing functional groups in RGO with Mn<sup>2+</sup> ions. The enhanced conductivity loss and interfacial polarization endowed MHSs-RGO hybrids with powerful dielectric loss capability. As a result, MHSs-RGO hybrids exhibited powerful RL of – 52.2 dB at 10.7 GHz and an ultra-wide EAB of 8.0 GHz with the thickness of 2.0 mm, which were significantly superior to those of most reported metal sulfides/carbon composites.

Among various transition metallic sulfides, two-dimensional transition metal dichalcogenides (2D TMDs) are an emerging class of MAMs with large surface areas, unique electronic properties, and multiple topological phases [84, 85]. Generally, 2D

TMDs are composed of X-M-X triple atom layers by van der Waals forces, which are structurally analogous to GO. Depending on the arrangement of X atoms, 2D TMDs layers can generate two distinct configurations: metallic 1T phase and semiconducting 2H phase. TMDs with pure 2H phase usually hold broadband gap and low carrier concentration, leading to their relatively poor conductivity. By contrast, 1T phase is proved to be metallic features with greatly enhanced conductivity, which is conducive to improving dielectric loss [86, 87]. Therefore, TMDs with 1T phase or mixed-phase of 1T and 2H have been considered as attractive candidates for the construction of new MAMs by combining with carbon materials. For example, Piao et al. designed urchin-like 1T-WS<sub>2</sub> nanosheets/single-walled CNTs (1T-WS<sub>2</sub>@SWCNTs) hybrid composites, and revealed that the minimum RL value could reach up to – 66.0 dB at 8.3 GHz with a matching thickness of 2.2 mm [88]. Guo et al. also showed that the microwave absorption performance of rose-like 1T@2H MoS<sub>2</sub>/RGO composites was significantly better than that of 2H-MoS<sub>2</sub>/RGO, due to the controllable crystalline phase switch between 2H and 1T [89]. These results demonstrate that a rational optimization on crystalline phase may also play an important role in improving EM functions of 2D TMDs/carbon composites.

Thanks to the morphology feature of 2D TMDs, many researchers devote their efforts to the microstructure of 2D TMDs/carbon composites. The archived references indicate that there are two kinds of microstructures quite favorable for microwave

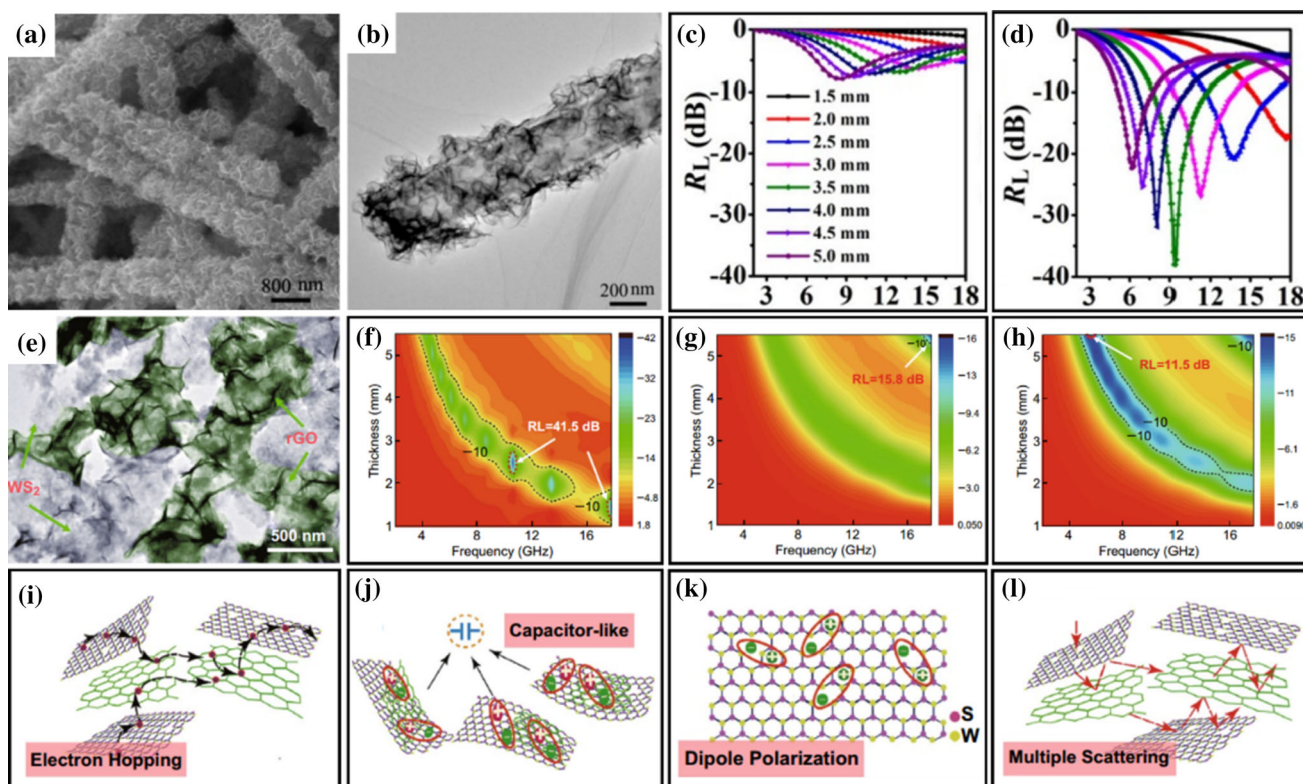


**Figure 3** SEM (a) and TEM (b) images of MoS<sub>2</sub> nanosheets/N-doped CNTs composites. RL curves of pure MoS<sub>2</sub> nanosheets (c) and MoS<sub>2</sub> nanosheets/N-doped CNTs composites (d) with varying absorber thicknesses. Adapted from Ref. [93], Copyright: 2018 American Chemical Society. Used with permission. TEM image of WS<sub>2</sub>-RGO (e). RL maps of WS<sub>2</sub>-RGO (f), pure RGO

(g), and pure WS<sub>2</sub> nanosheets (h). Synergistic mechanisms responsible for the superior microwave absorption properties of WS<sub>2</sub>-RGO: electron hopping (i), interfacial polarization (j), dipole polarization (k), and multiple reflection and scattering of incident EM waves (l). Adapted from Ref. [97], Copyright: 2019 Springer. Used with permission.

absorption. One is to induce the perpendicular growth of 2D TMDs on the surface of carbon materials [90–92]. As shown in Fig. 3a, b, Liu et al. modified thin MoS<sub>2</sub> nanosheets vertically on the surface of ultra-long N-doped CNTs by anion-exchange reaction [93]. Compared with pure MoS<sub>2</sub> nanosheets (minimum RL of -10.0 dB) (Fig. 3c), the as-prepared composite displayed a remarkable enhancement in microwave absorption performance, whose minimum RL value could reach -38.3 dB at frequency of 9.4 GHz (Fig. 3d). EM analysis indicated that loose 2D TMDs not only facilitated the entry of EM waves, but also promoted their multiple reflections, thus accelerating the consumption of EM energy. On the other hand, it is also of great interest to design a face-to-face microstructure with 2D TMDs and RGO, because such a configuration with sufficiently contacted areas can provide more charge transmission channels and shorten charge migration distance, resulting in a higher charge transfer rate

[94–96]. For example, Zhang et al. successfully synthesized WS<sub>2</sub>/RGO composites with typical face-to-face configuration (Fig. 3e), which displayed superior EM waves attenuation capability as well as impedance matching characteristics to those of pure RGO or WS<sub>2</sub> nanosheets (Fig. 3f-h) [97]. The significant enhancement of microwave absorption could be attributed to the following aspects: first, the transfer and hopping of electrons between heterogeneous nanosheets endowed the composite with enhanced conductivity loss; second, due to the difference in the surface conductivity of RGO and WS<sub>2</sub>, the accumulation and rearrangement of local charges might lead to interfacial polarization; third, a large number of defects in WS<sub>2</sub> and RGO layers would act as dipoles to enhance dipole oriented polarization; fourth, unique 2D lamellar structure of WS<sub>2</sub>-RGO nanosheets brought high specific surface area and plenty of interlayer voids, promoting multiple reflection and scattering of EM waves (Fig. 3i-l). Table 2 further

**Table 2** Microwave absorption performance of metal sulfides/carbon composites

Absorber	Minimum RL (frequency, thickness)	EAB at 2.0 mm (range)	Reference
MoS <sub>2</sub> @hollow carbon spheres	– 65.0 dB (10.3 GHz, 2.0 mm)	3.0 GHz (9.0–12.0 GHz)	[27]
SnS/GO	– 41.2 dB (12.9 GHz, 3.2 mm)	0.9 GHz (17.1–18.0 GHz)	[76]
MWCNTs/CoS	– 56.1 dB (6.6 GHz, 3.6 mm)	4.2 GHz (11.0–15.2 GHz)	[80]
MHSs-RGO	– 52.2 dB (10.7 GHz, 2.5 mm)	8.0 GHz (10.0–18.0 GHz)	[83]
2D MoS <sub>2</sub> /graphene	– 41.9 dB (16.1 GHz, 2.4 mm)	3.9 GHz (14.1–18.0 GHz)	[85]
WS <sub>2</sub> /SWCNTs	– 66.0 dB (8.3 GHz, 2.2 mm)	2.1 GHz (8.4–10.5 GHz)	[88]
1T@2H-MoS <sub>2</sub> /RGO	– 67.8 dB (10.4 GHz, 2.5 mm)	4.0 GHz (11.6–15.6 GHz)	[89]
WS <sub>2</sub> /CNTs	– 51.6 dB (14.8 GHz, 2.0 mm)	5.4 GHz (12.6–18.0 GHz)	[92]
MoS <sub>2</sub> /N-doped CNTs	– 38.3 dB (9.4 GHz, 3.5 mm)	2.9 GHz (15.1–18.0 GHz)	[93]
2D MoS <sub>2</sub> /RGO	– 55.0 dB (12.3 GHz, 2.6 mm)	3.5 GHz (14.5–18.0 GHz)	[94]
2D WS <sub>2</sub> -RGO	– 41.5 dB (9.5 GHz, 2.7 mm)	3.2 GHz (12.0–15.2 GHz)	[97]
In <sub>2</sub> S <sub>3</sub> @CNTs	– 42.8 dB (12.0 GHz, 1.6 mm)	4.2 GHz (7.3–11.5 GHz)	[98]
MoS <sub>2</sub> /RGO	– 50.9 dB (11.7 GHz, 2.3 mm)	5.7 GHz (11.7–17.4 GHz)	[99]
MnS <sub>2</sub> /CNTs	– 63.8 dB (17.4 GHz, 1.4 mm)	3.6 GHz (10.0–13.6 GHz)	[100]
CoS-RGO	– 54.2 dB (6.8 GHz, 4.0 mm)	4.0 GHz (12.1–16.1 GHz)	[101]
MoS <sub>2</sub> /graphene	– 57.3 dB (11.0 GHz, 2.6 mm)	4.8 GHz (12.8–17.6 GHz)	[102]

provides the comparisons in RL intensity and EABs of various metal sulfides/carbon composites. These composites also display considerable RL intensity like those metal oxides/carbon composites, while their EABs are more or less broadened as compared with metal oxides/carbon composites. This phenomenon may be attributed to the fact that metal sulfides can generate better conductivity loss. In some rare cases, MHSs-RGO even demonstrates its very broad EAB up to 8.0 GHz, suggesting that rational manipulation on microstructure and heterogeneous interface will be an important development direction for metal oxides/carbon composites.

### Conductive polymers/carbon composites

Due to the unusual electronic properties gifted by extended  $\pi$ -conjugated system, conductive polymers, known as “synthetic metal”, exhibit higher electrical conductivity than metal oxides and metal sulfides, which render them as promising MAMs [103, 104]. Although conductive polymers were initially utilized as EM shielding materials, some researchers noticed that their good shielding effectiveness was not completely established on reflection principle, but also contributed by their microwave absorption [105–108]. This finding has inspired a lot of research work to develop novel MAMs based on various conductive

polymers, including conductive polymers/magnetic metals, conductive polymers/metal oxides, conductive polymers/metal sulfides, conductive polymers/carbon materials, and so on [109–112]. Among them, the composites of conductive polymers and carbon materials are considered as one of the most promising MAMs for practical applications because of their additional advantages in lightweight, flexibility, and low cost [113, 114]. For example, when carbon black or graphite was coated with an appropriate amount of polyaniline (PANI), the microwave absorption efficiencies of the obtained composites were obviously higher than those of individual components [115, 116].

Since the discovery of CNTs, they received much more attention than conventional carbon black or graphite in the construction of conductive polymers/carbon composites, because their unique one-dimensional (1D) microstructure was quite favorable for electron transfer and the formation of conductive networks [117]. Sharma et al. demonstrated that dielectric loss capability of PANI-CNTs films was obviously stronger than that of pure PANI films as a result of the interaction between PANI molecular chains and surface functional groups of CNTs [118]. Ting et al. also found that the EM parameters of PANI/MWCNTs composites could be easily manipulated by adjusting the weight ratio of MWCNTs to PANI and confirmed that PANI/MWCNTs



composites could obtain ultra-wideband microwave absorption when the weight ratio was optimized [119]. However, it has to point out that the dispersion of CNTs is usually poor, and thus there still remains a challenge to conduct the polymerization of various monomers on the external surface of CNTs uniformly. In many cases, the polymerization of various monomers may result in the formation of individual conductive polymers [120, 121]. Wang et al. ever unzipped CNTs with a series of strongly oxidative processes, and they found that PANI layer with tailorable thickness could be homogeneously coated on the surface of partially unzipped CNTs (Fig. 4) [122]. Undoubtedly, the strongly oxidative treatment

generated rich functional groups on the surface of CNTs, which boosted the interaction between CNTs and aniline monomers, finally accounting for the homogeneous PANI layer. More importantly, they further validated that once the 1D microstructure of CNTs was thoroughly destroyed, the microwave absorption performance of CNTs/PANI composites will be drastically degraded. In addition, plasma pretreatment has also been proved to be an effective strategy for preparing homogeneous CNTs/PANI composites [123], because plasma pretreatment in the presence of O<sub>2</sub> could create a large number of oxygen radicals that was responsible for the grafting of more aniline monomers. This pretreatment not only

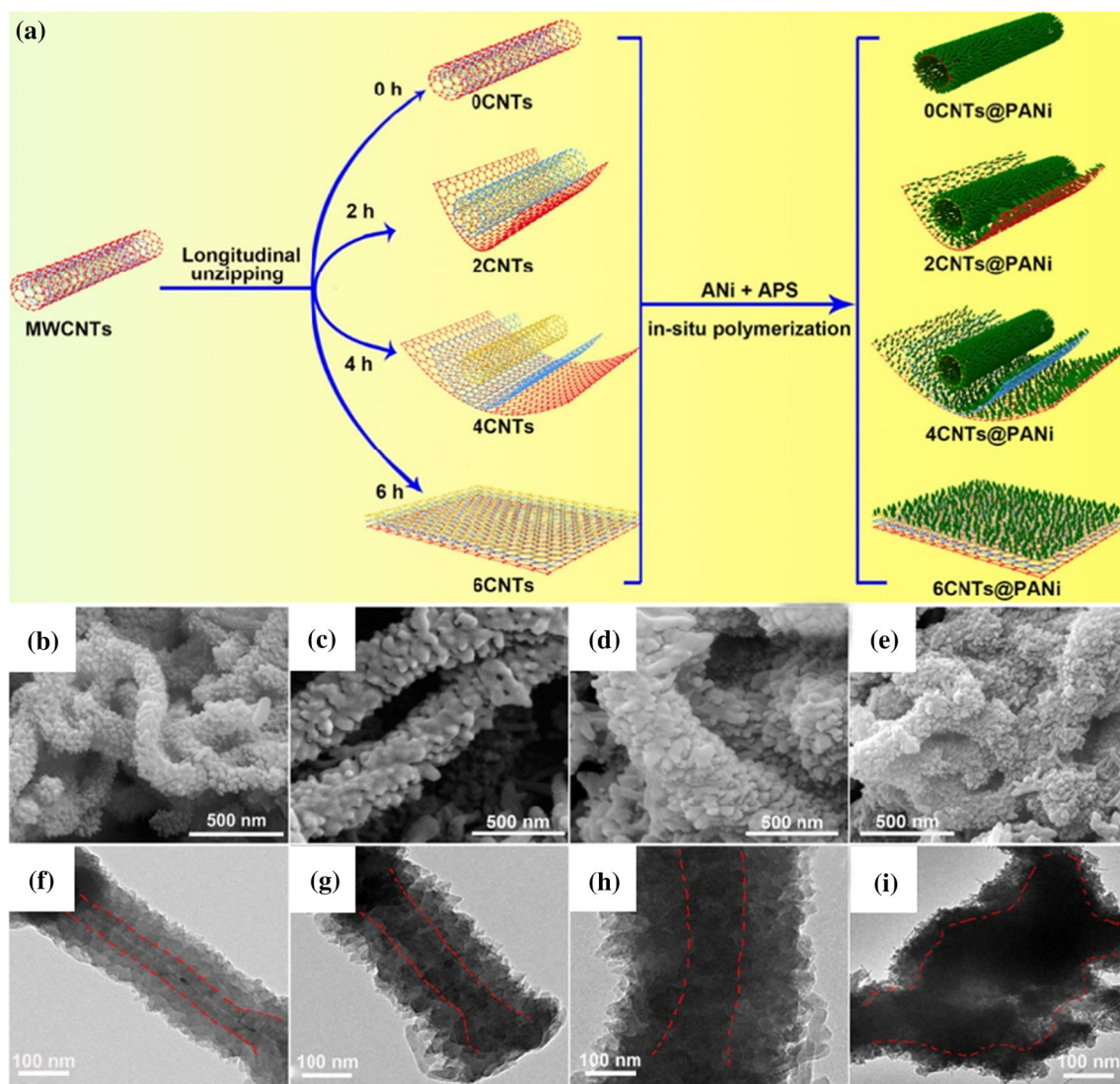


**Figure 4** Schematic illustration of the preparation of oxidation-peeled CNTs@PANI hybrids (a). SEM and TEM images of CNTs@PANI hybrids with different oxidation peeling time of 0 h

(b and f), 2 h (c and g), 4 h (d and h), and 6 h (e and i). Adapted from Ref. [122], Copyright: 2019 American Chemical Society. Used with permission.

worked for the good homogeneity of CNTs/PANI composites, but also contributed to their dielectric loss capabilities.

The successful peeling off of graphite makes graphene and graphene oxide (GO) burgeoning members in carbon family [124]. First-principle calculations also demonstrate that they can be tightly coupled with conductive polymers through strong  $\pi$ - $\pi$  interaction [125]. On one hand, it contributes to the structural stability of conductive polymers/graphene composites. On the other hand, it may promote hybridization and charge transfer between conductive polymers and graphene sheets, and enhance dipole orientation polarization. These advantages endow conductive polymers/graphene composites with immense potential for overcoming the challenges related to durability and performance in the field of microwave absorption. Yu et al. pioneered a perpendicular growth of PANI nanorods on the surface of graphene and the PANI nanorod arrays produced a significant improvement in microwave absorption properties, including strong RL ( $-45.1$  dB) and broad EAB at 2.0 mm (4.3 GHz) [126]. Both theoretical simulation and experimental results suggested that the good microwave absorption performance of PANI/graphene composite was attributed to the profitable synergistic effect between graphene and PANI nanorods. Very interestingly, Chen et al. proposed an in situ intercalation polymerization to prepare PANI/graphene composites to avoid pre-peeling off of graphite [127]. As shown in Fig. 5a, b, the intercalation of aniline cation into bilayer graphene was an energetically favorable reaction with calculated formation energy of 2.81 eV, and the intercalated aniline cation could weaken the interactions between the interlamellations and account for larger interlamellar space. When the polymerization of aniline cation was triggered, the macromolecular organic chain and the exothermal effect would drive a violent separation of graphite interlayers. The final composite presented its minimum RL of  $-36.9$  dB at 10.3 GHz, and the corresponding bandwidth less than  $-10.0$  dB was 5.3 GHz (from 8.2 to 13.5 GHz) with an absorber thickness of 3.5 mm (Fig. 5c). It is noteworthy that more and more researchers are interested in various conductive polymers/graphene composites, such as sandwich-like PANI/GO composites [128], graphene sheets/poly(3,4-ethylenedioxythiophene) (PEDOT) nanofibers [129], polypyrrole (PPy) nanosphere/RGO

composites [130]. On the basis of these studies, Wu et al. further employed 3D RGO aerogel as the scaffold for PEDOT/RGO composites, and they realized ultra-broad effective absorption by manipulating the absorber thickness [131]. The microwave absorption properties of some conductive polymers/carbon composites are listed in Table 3. As observed, there are more composites that can produce both strong RL intensities and broad EABs. It is worth noting that the composite with PANI layer and partially unzipped CNTs gives the best EAB with the absorber thickness of 2.0 mm, which suggests that the graft of aniline monomers on CNTs before their polymerization will be greatly helpful to promote the interaction between PANI and CNTs, finally boosting the microwave absorption performance.

### Carbides/carbon composites

Although metal oxides/sulfides and conductive polymers can greatly promote microwave absorption performance of carbon-based composites, some intrinsic drawbacks, e.g. easy corrosion and naturally faded dielectric property, will restrain their practical applications to some extent, especially under some rigorous conditions [136]. Therefore, it still remains a challenge to construct durable and high-performance carbon-based dielectric composites for microwave absorption. As typical dielectric ceramics, carbides with favorable features of corrosion resistance, oxidation resistance, and polarization relaxation show their distinct advantages as secondary dielectric components in carbon-based composites [137, 138]. Silicon carbide (SiC) is one of the most common carbides that are applied in the field of microwave absorption [139, 140]. Baskey et al. investigated the dielectric properties of SiC/exfoliated graphite composites, and they found that even though these composites were just fabricated by simple physical mixing, a significant enhancement in microwave absorption performance could be easily manifested in X band [141]. As we all know, conventional carbides are always generated at high temperature ( $> 1000$  °C), which means rational design on their microstructure will be quite difficult. In an effort to achieve better performance, several groups tend to choose carbon foam as a scaffold to support SiC particles or fibers [142, 143]. This combination model not only favors the synergistic effect between SiC

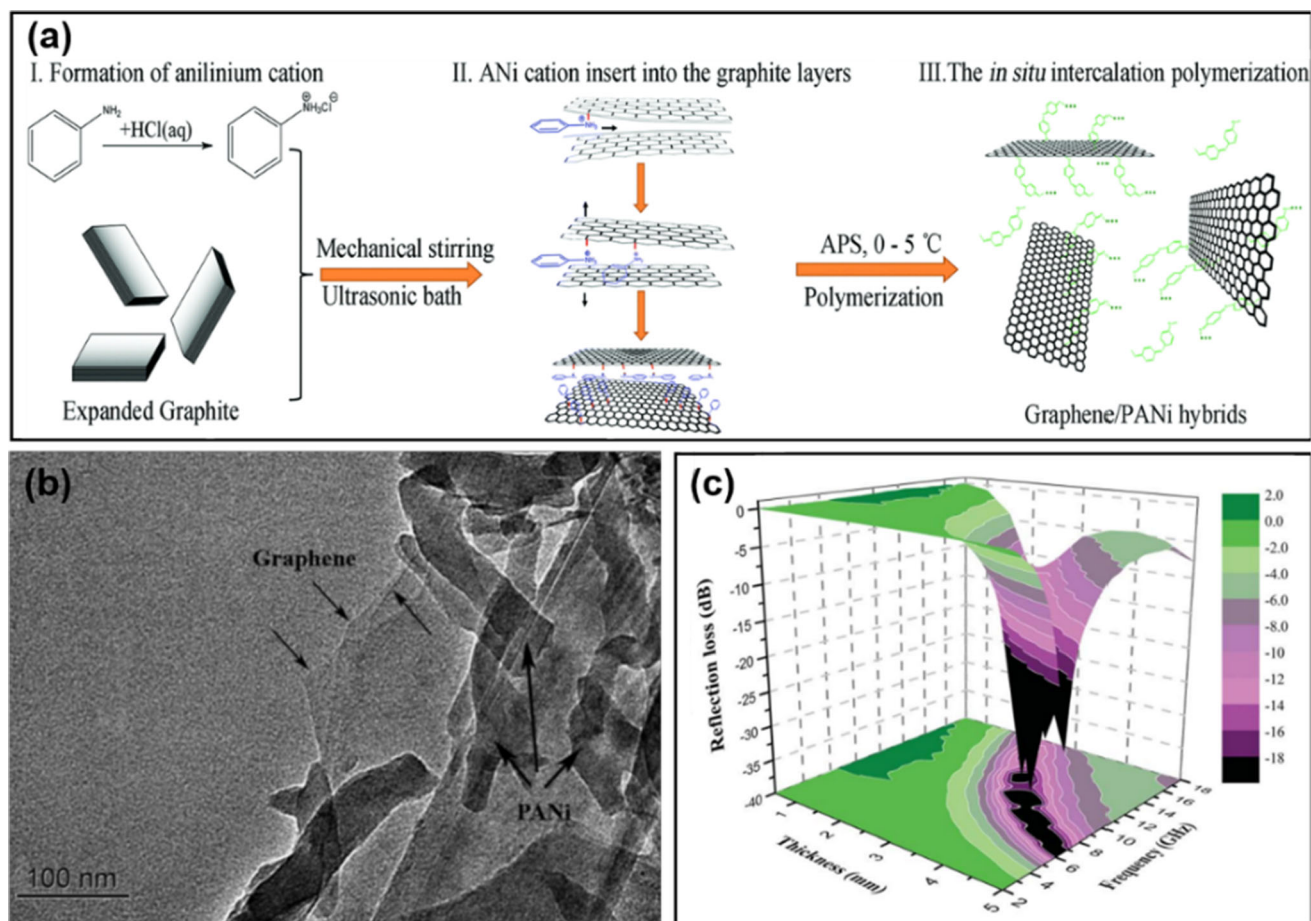


**Figure 5** Schematic illustration for the intercalation polymerization of ANI<sup>+</sup> into expanded graphite to synthesize PANI/graphene hybrids (a). TEM image (b) and 3D map of

calculated RL values (c) for PANI/graphene hybrids. Adapted from Ref. [127], Copyright: 2014 Royal Society of Chemistry. Used with permission.

particles and carbon substrate, but also introduces multiple reflections and polarization relaxations [144, 145].

The advent of MXenes has announced a kind of new 2D metal carbides to the world [146–148]. The unique 2D laminated structure, excellent electrical conductivity, active surface functional groups, and native defects render them as promising MAMs [149, 150], which also promote the development of carbides/carbon composites to a great extent [151, 152]. The decoration of MXenes with carbon nanomaterials, such as carbon nanospheres and CNTs, has been demonstrated as an effective strategy to produce good microwave absorption performance in carbides/carbon composites [153, 154]. However, the closely packed MXenes nanosheets cannot provide sufficient interaction with carbon materials, and thus the construction of carbon-based composites with few-layered MXenes is becoming a hot topic in

the related field [155]. For example, Li et al. designed core-shell graphene-bridged hollow MXenes spheres as lightweight MAMs [156]. The specific preparative process is schematically depicted in Fig. 6a. Few-layered Ti<sub>3</sub>C<sub>2</sub>T<sub>x</sub> MXenes (2–8 layers) from selective centrifugation were firstly assembled with polymethyl methacrylate (PMMA) nanospheres through hydrogen bonding and Van der Waals force, and then the as-obtained hybrids were wrapped with GO nanosheet and heated at 450 °C under Ar atmosphere. The final composite was not only very active in X band with the absorber thickness of 3.2 mm, but also displayed a very attractive feature with ultra-low density (0.0033 g/cm<sup>3</sup>, Fig. 6b, c). Zhou's group found that few-layered GO and Ti<sub>3</sub>C<sub>2</sub>T<sub>x</sub> MXenes could ingeniously assemble into a face-to-face heterogeneous structure by hydrogen bonding interaction [157], and they injected GO/Ti<sub>3</sub>C<sub>2</sub>T<sub>x</sub> MXenes solution into liquid nitrogen with a Taylor Cone.



**Table 3** Microwave absorption performance of conductive polymers/carbon composites

Absorber	Minimum RL (frequency, thickness)	EAB at 2.0 mm (range)	Reference
RGO-PANI	− 41.4 dB (13.8 GHz, 2.0 mm)	4.2 GHz (11.7–15.9 GHz)	[113]
PANI/expanded graphite	− 32.0 dB (9.7 GHz, 3.0 mm)	Unshown	[116]
MCNTs@PPy	− 44.0 dB (8.5 GHz, 4.0 mm)	2.0 GHz (16.0–18.0 GHz)	[120]
PEDOT/SWCNT	− 43.0 dB (9.4 GHz, 3.0 mm)	5.3 GHz (12.5–17.8 GHz)	[121]
CNTs@PANI	− 45.7 dB (12.0 GHz, 2.4 mm)	5.6 GHz (12.4–18.0 GHz)	[122]
CNTs/PANI	− 41.4 dB (13.3 GHz, 2.0 mm)	8.3 GHz (9.7–18.0 GHz)	[123]
Graphene-based PANI	− 32.1 dB (5.5 GHz, 4.0 mm)	5.7 GHz (10.2–15.9 GHz)	[125]
Graphene/PANI	− 45.1 dB (12.9 GHz, 2.5 mm)	4.3 GHz (13.7–18.0 GHz)	[126]
Graphene/PANI	− 36.9 dB (10.3 GHz, 3.5 mm)	–	[127]
PANI/GO	− 41.3 dB (6.8 GHz, 5.0 mm)	0.3 GHz (1.7–2.0 GHz)	[128]
Graphene-PEDOT	− 48.1 dB (10.5 GHz, 2.0 mm)	3.1 GHz (9.2–12.3 GHz)	[129]
PPy/RGO	− 59.2 dB (5.0 GHz, 3.8 mm)	2.8 GHz (9.1–11.9 GHz)	[130]
3D-RGO/PEDOT	− 35.5 dB (13.4 GHz, 2.0 mm)	5.0 GHz (11.5–16.5 GHz)	[131]
Hollow carbon@PANI	− 64.0 dB (11.1 GHz, 2.5 mm)	2.5 GHz (13.8–16.3 GHz)	[132]
PPy@C	− 38.1 dB (11.6 GHz, 3.0 mm)	1.1 GHz (10.6–11.7 GHz)	[133]
PPy/GO	− 58.1 dB (12.4 GHz, 3.0 mm)	1.2 GHz (16.8–18.0 GHz)	[134]
Graphene/PANI	− 52.5 dB (13.8 GHz, 2.0 mm)	4.2 GHz (11.8–16.0 GHz)	[135]

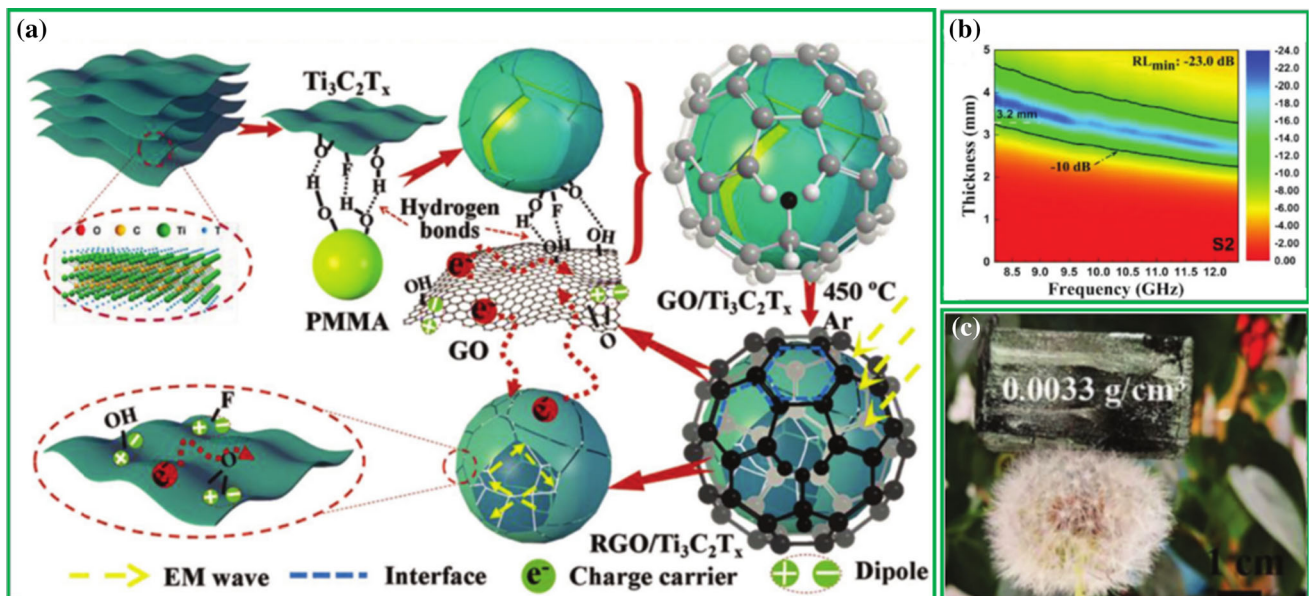


**Figure 6** Schematic illustration of the preparation of RGO/Ti<sub>3</sub>C<sub>2</sub>T<sub>x</sub> foam (a). RL map (b) and photograph (c) for RGO/Ti<sub>3</sub>C<sub>2</sub>T<sub>x</sub> foam. Adapted from Ref. [156], Copyright: 2018 Wiley. Used with permission.

After freeze drying, Ti<sub>3</sub>C<sub>2</sub>T<sub>x</sub> MXene@GO hybrid aerogel microspheres could be finally generated, and these aerogel microspheres even produced effective microwave absorption in S band (− 38.3 dB at 2.1 GHz). In addition, Ti<sub>3</sub>C<sub>2</sub>T<sub>x</sub> MXenes were also widely coupled with 3D RGO aerogels, and with the advantages of 3D microstructure, these composites

could work for the attenuation of incident EM waves in 4.0–18.0 GHz by manipulating the absorber thickness [158].

It is undoubted either conventional SiC or emerging MXenes will be helpful to enhance microwave absorption performance of carbon-based composites, while their very large particle/sheet size may bring



two shortcomings in carbides/carbon composites. One is the relatively poor chemical homogeneity, which is not favorable for good functional reproducibility in practical application [159]. The other is the insufficient contact between carbides and carbon materials. Interfacial polarization originating from the uneven distribution of space charges is always considered as one of the main pathways to consume EM energy [160], and thus the insufficient contact between carbides and carbon materials implies there is still room for performance upgradation. As compared with SiC and MXenes, molybdenum carbide ( $\text{Mo}_2\text{C}$ ) may be generated at much lower temperature (600–800 °C vs. 1000–1600 °C), that is to say,  $\text{Mo}_2\text{C}$  usually has much smaller particle size (ca. 5–20 nm) than SiC and MXenes [161–163]. To date,  $\text{Mo}_2\text{C}$  has been established as a promising substitute for SiC and MXenes to combine with carbon materials for microwave absorption [164]. For example, Dai et al. pioneered the synthesis of porous-carbon-based  $\text{Mo}_2\text{C}$  nanocomposites with Cu-Mo-based MOFs as the precursor [165], and they found  $\text{Mo}_2\text{C}$  nanoparticles about 20 nm were uniformly dispersed in porous carbon octahedrons. The synergistic effect between  $\text{Mo}_2\text{C}$  nanoparticles and carbon octahedrons was confirmed to be highly contributive to excellent

dielectric properties, resulting in strong RL (−49.0 dB at 9.0 GHz) and broad effective bandwidth (4.6 GHz) with the absorber thickness of 1.7 mm. Our group improved the synthesis of  $\text{Mo}_2\text{C}/\text{C}$  composites by employing Mo-substituted ZIF-8 as a self-sacrificing template (Fig. 7a) [166]. We successfully decreased the average size of  $\text{Mo}_2\text{C}$  nanoparticle to about 4.5 nm (Fig. 7b), and the corresponding RL intensity and effective response bandwidth were raised to −60.4 dB and 4.8 GHz, respectively, even with a smaller absorber thickness (1.5 mm, Fig. 7c). More importantly, these  $\text{Mo}_2\text{C}/\text{C}$  composites exhibited durable microwave absorption performance, and oxidation treatment (473 K for 24 h) and acidic etching (3.0 mol/L of HCl for 24 h) hardly changed their RL characteristics. In our latest research, we demonstrated a solvent-free strategy to produce tungsten carbide/carbon composites for microwave absorption, where ultra-fine cubic tungsten carbide nanoparticles homogeneously decorated on carbon nanosheets were simply achieved by the direct pyrolysis of dicyandiamide/ammonium metatungstate mixture [167]. The optimized composite could produce comparable performance (minimum RL of −55.6 dB with the absorber thickness of only 1.3 mm) to those  $\text{Mo}_2\text{C}/\text{C}$  composites

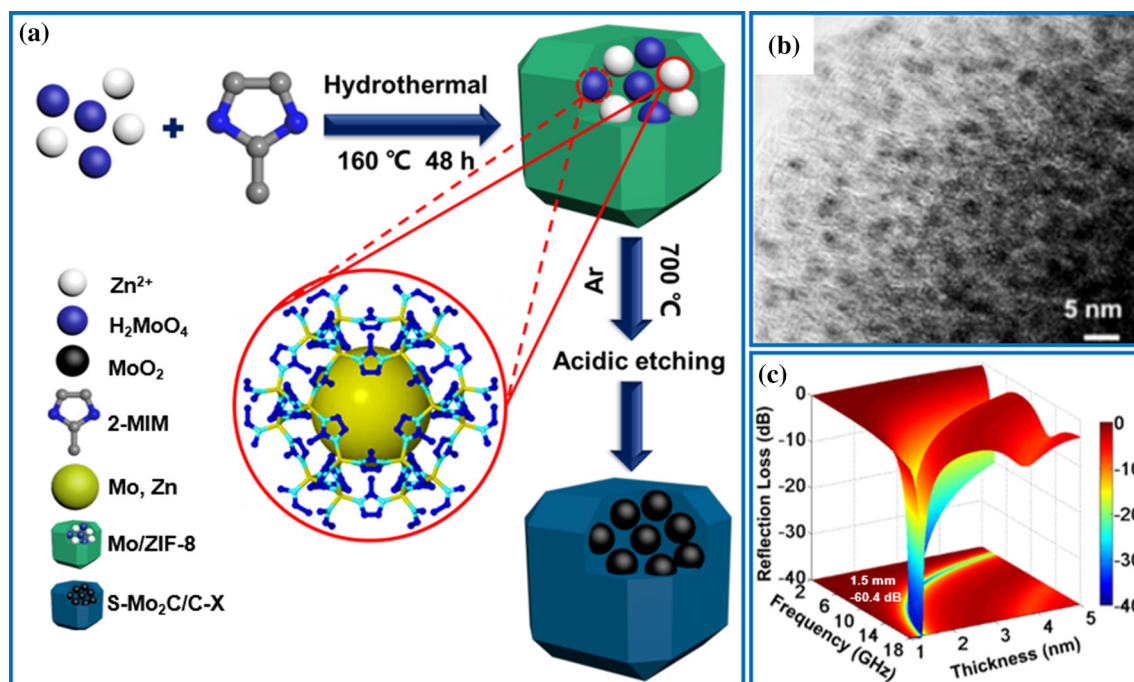


**Figure 7** Schematic illustration of preparing  $\text{Mo}_2\text{C}/\text{C}$  composites (a). TEM image (b) and 3D map of calculated RL values (c) for  $\text{Mo}_2\text{C}/\text{C}$  composites. Adapted from Ref. [166], Copyright: 2018 American Chemical Society. Used with permission.

**Table 4** Microwave absorption performance of carbides/carbon composites

Absorber	Minimum RL (frequency, thickness)	EAB at 2.0 mm (range)	Reference
Activated carbon felt@B <sub>4</sub> C	− 36.1 dB (17.2 GHz, 5.0 mm)	1.2 GHz (14.3–15.5 GHz)	[26]
Graphite/SiC	− 22.0 dB (16.8 GHz, 1.7 mm)	5.5 GHz (12.5–18.0 GHz)	[136]
SiC whiskers@C	− 61.2 dB (9.0 GHz, 4.2 mm)	2.7 GHz (15.3–18.0 GHz)	[137]
B <sub>4</sub> C@C	− 60.8 dB (15.5 GHz, 1.5 mm)	3.3 GHz (9.3–12.6 GHz)	[138]
SiC/C foam	− 20.0 dB (14.0 GHz, 3.0 mm)	Unshown	[143]
SiC/C foam	− 51.6 dB (9.0 GHz, 3.6 mm)	4.0 GHz (14.0–18.0 GHz)	[144]
SiC nanowire/C foam	− 31.2 dB (15.8 GHz, 1.5 mm)	2.6 GHz (10.6–13.2 GHz)	[145]
Graphene/Ti <sub>3</sub> C <sub>2</sub>	− 52.0 dB (13.3 GHz, 1.4 mm)	1.7 GHz (6.9–8.6 GHz)	[151]
Ti <sub>3</sub> C <sub>2</sub> T <sub>x</sub> MXenes/carbon sphere	− 54.7 dB (4.0 GHz, 4.8 mm)	2.8 GHz (10.5–13.3 GHz)	[153]
Ti <sub>3</sub> C <sub>2</sub> T <sub>x</sub> /CNT	− 52.9 dB (7.2 GHz, 2.7 mm)	3.4 GHz (9.5–12.9 GHz)	[154]
Ti <sub>3</sub> C <sub>2</sub> T <sub>x</sub> MXene@GO	− 49.1 dB (14.2 GHz, 1.2 mm)	3.6 GHz (6.6–10.2 GHz)	[157]
Ti <sub>3</sub> C <sub>2</sub> T <sub>x</sub> MXene@RGO	− 31.2 dB (8.2 GHz, 3.1 mm)	5.5 GHz (11.3–16.8 GHz)	[158]
Mo <sub>2</sub> C@C	− 48.0 dB (12.5 GHz, 1.9 mm)	4.1 GHz (10.1–14.2 GHz)	[164]
Mo <sub>2</sub> C/C	− 49.2 dB (9.0 GHz, 2.6 mm)	4.2 GHz (10.6–14.8 GHz)	[165]
Mo <sub>2</sub> C/C	− 60.4 dB (15.0 GHz, 1.5 mm)	3.0 GHz (9.6–12.6 GHz)	[166]
WC <sub>1−x</sub> /C	− 55.6 dB (17.5 GHz, 1.3 mm)	3.6 GHz (9.6–13.2 GHz)	[167]

from complex liquid-phase/solvothermal reactions, providing a new and green method for carbides/carbon composites. Table 4 presents microwave absorption properties of various carbides/carbon composites. Although carbides/carbon composites are very stable as compared with other kinds of composites, they seem more or less inferior in RL intensity and EAB, and the best candidate in this series only gives EAB value at 5.5 GHz. This situation means that it still remains a challenge in reinforcing their microwave absorption performance through rational design in composition and microstructure. In addition, most studies focus on SiC and Ti<sub>3</sub>C<sub>2</sub>T<sub>x</sub>-MXenes, and Mo<sub>2</sub>C or other carbides with ultra-fine particle size may be the new choice for carbides/carbon composites.

### Carbon/carbon composites

According to classical dielectric theory, interfacial polarization, as a main pathway for energy loss, may occur at any interface with different accumulation states of space charges [168, 169]. Even for the materials with the same chemical composition, if they have different crystalline structures, positive interfacial polarization will still take place at their interfaces. This criterion therein drives the development of carbon/carbon composites as novel MAMs, because

their chemical stability is as good as that of carbides/carbon composites, but without involving any metal composition [170]. Singh et al. planted CNTs on carbon fibers via a catalytic chemical vapor deposition method, and numerous capacitor-like structures at the interfaces between CNTs and carbon fibers might enhance polarization loss and induce dipole polarization, and more importantly, they also created unique trapping centers for multiple reflections and scatterings [171]. Zhang et al. found that the carbonization of polyacrylonitrile (PAN) nanofibers under ammonia atmosphere would lead to the formation of heterogeneous structures between porous carbon nanofibers (CNFs) and CNTs, because the carbonized PAN nanofibers could be etched by gaseous CH<sub>4</sub> and some radicals (i.e. NH<sub>2</sub>, NH, and H), and these etching pores further played as the nucleation sites for the growth of CNTs [172]. This complex architecture indeed promoted the consumption of EM energy and endowed such a carbon/carbon composite with some advantages in lightweight and strong absorption.

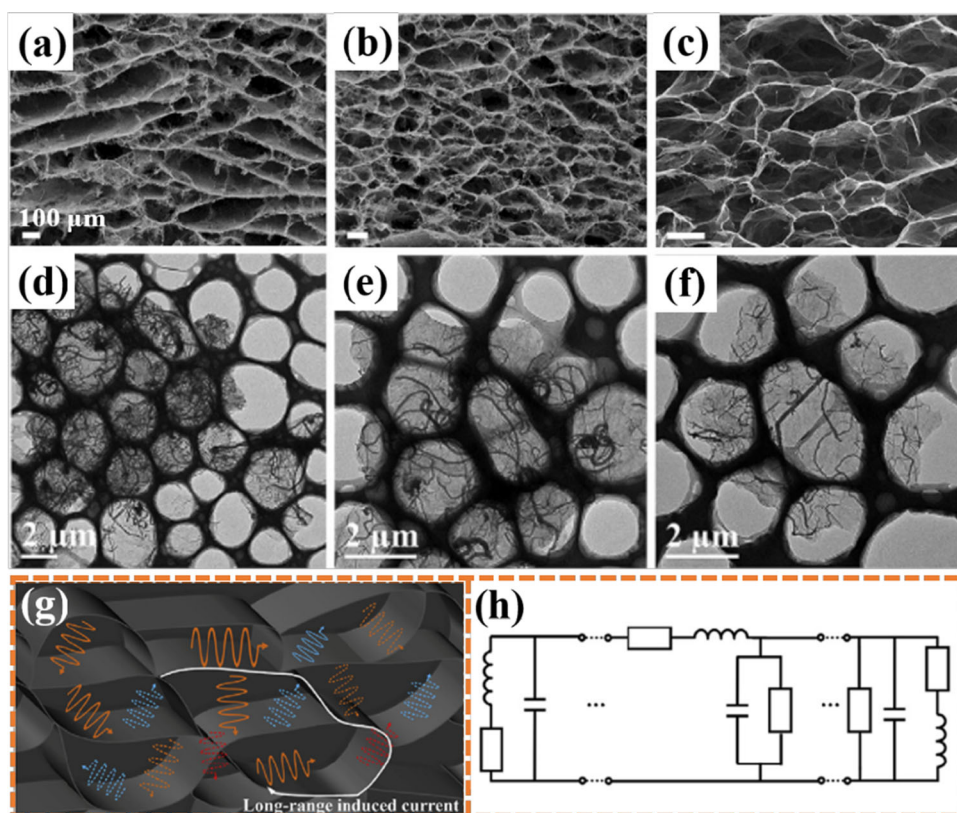
Since the successful peeling of carbon monolayer from graphite, graphene became one of the most popular candidates in various carbon/carbon composites, because its unique 2D structure can be considered as an ideal platform for the growth or deposition of secondary carbon components [173]. For example, Tang et al. attached carbon black

particles on the surface of RGO and demonstrated that minimum RL of the as-synthesized composites was as strong as  $-47.5$  dB, and their EAB could reach up to  $5.9$  GHz with the thickness of only  $2.2$  mm. This result confirmed that a significant enhancement in microwave absorption could be easily achieved through this simple combination [174]. Zhang et al. wrapped CNFs with RGO, and the synergistic effects in this binary composite greatly contributed to microwave attenuation performance, where CNFs could afford desirable conductivity loss with an extremely long conductive network and RGO could generate multiple polarizations at a moderate amount of defect sites [175]. As we mentioned above, microstructure design is also an important aspect that should be taken into account for microwave absorption. Therefore, 3D RGO aerogel is widely considered as the first choice for carbon/carbon composites in the latest studies [176]. Figure 8a–f shows SEM and TEM images of MWCNTs/graphene foams with different mass ratios [177]. It is clear that a solvothermal process not only assembles RGO sheets into reticulum-like open cell structure with average pore size less than  $100$   $\mu\text{m}$ , but also realizes good dispersion of MWCNTs on the surface of RGO sheets.

When these foams are placed in an external EM field, they will create extremely long and complex transmission channels for incident EM waves, and work as massive resistance-inductance-capacitance coupled circuits and generate time-varying EM fields-induced currents, thus consolidating microwave absorption performance (Fig. 8g, h).

Of note is that either carbon black particles or CNTs have good crystallinity, i.e. high graphitization degree similar to that of RGO, which means that they are incapable of establishing a remarkable gradient in space charge accumulation at their interfaces, and thus the contribution from interfacial polarization is still much less than we expected. An effective strategy to fulfill powerful interfacial polarization is the combination of crystalline carbon materials and amorphous carbon materials [178]. For instance, Li winded hollow mesoporous carbon microspheres with CNTs, and the existence of CNTs accounted for the positive increases in conductive loss from  $0.12$  to  $2.27$  and polarization loss from  $0.15$  to  $0.67$  [179]. Our group previously designed a sandwich-like carbon/carbon composite with amorphous carbon microspheres (ACMs) and RGO through electrostatic interaction (Fig. 9a, b) [180]. Simulation results

**Figure 8** SEM and TEM images of MWCNT/graphene foams with the mass ratio of MWCNT to graphene of 1:2 (a and d), 1:3 (b and e), and 1:7 (c and f). Schematic illustration of the extremely long and complex transmission channels for the incoming EM waves (g) and the formation of resistance-inductance-capacitance coupled circuits in MWCNT/graphene foams (h). Adapted from Ref. [177], Copyright: 2017 Elsevier. Used with permission.





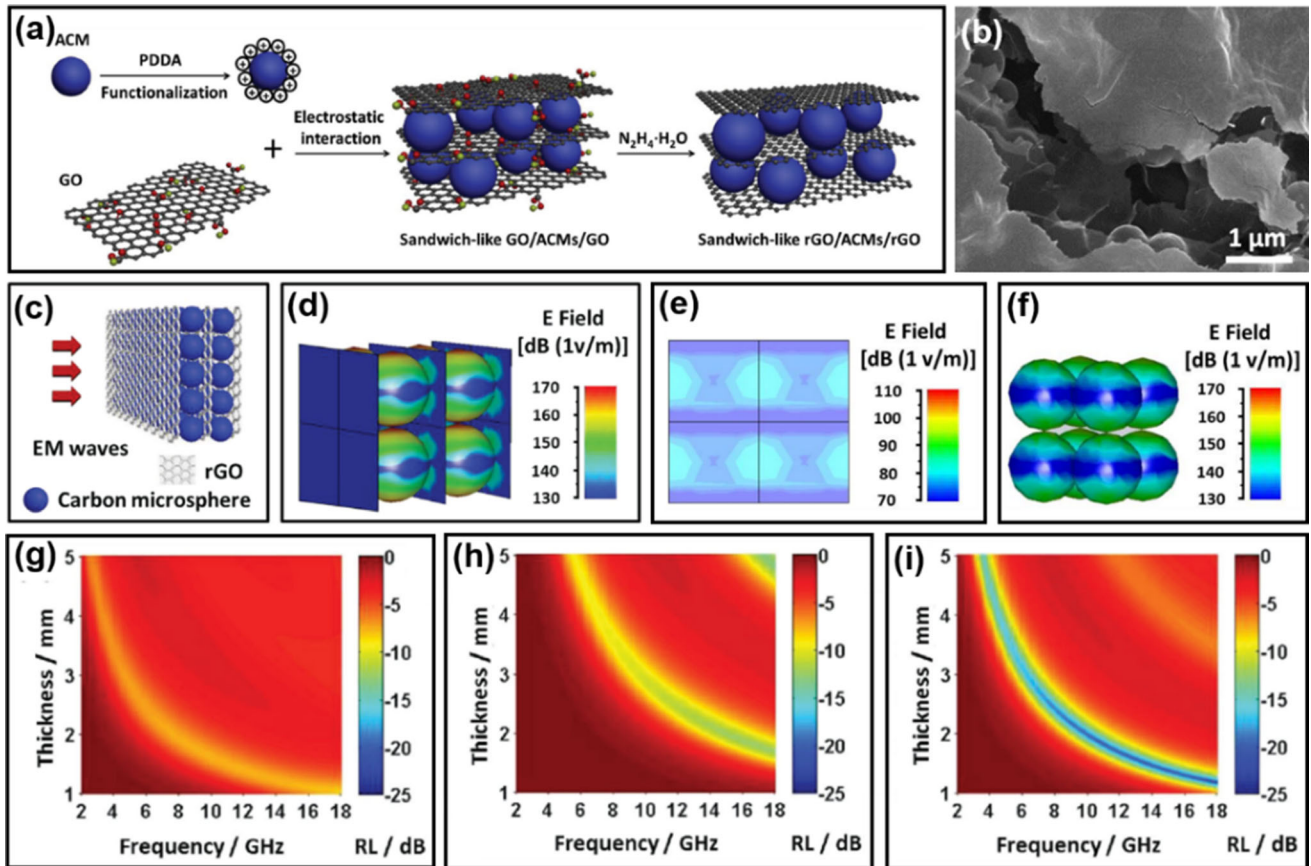


**Figure 9** Schematic illustration of preparation (a), SEM image (b), and simulation model (c) of sandwich-like RGO/ACMs/RGO composites. Electric field distributions of RGO/ACMs/RGO (d),

RGO (e), and ACMs (f). RL maps of RGO (g), ACMs (h), and RGO/ACMs/RGO (i). Adapted from Ref. [180], Copyright: 2016 Wiley. Used with permission.

revealed that there were two obviously enhanced electric field distributions in RGO/ACMs/RGO, one at the interfaces between ACMs and RGO, and the other at the spherical caps of ACMs along the vertical direction toward propagation of EM waves (Fig. 9c-f). It was proposed that the electric field distribution at the interfaces originated from the expected interfacial polarization, and the one at the spherical caps benefited from multiple reflections of EM waves induced by the separated RGO sheets. These significant improvements made RGO/ACMs/RGO more favorable for microwave absorption than individual RGO and ACMs (Fig. 9g-i). In the following study, we also decorated RGO with carbon nanopolyhedrons (CNPs) through in situ pyrolysis of ZIF-8/GO hybrids [181]. EM analysis again manifested that interfacial polarization was a critical factor to produce good microwave absorption performance. When the loading content of CNPs was tailored, the optimized CNPs/RGO would display strong RL

(− 66.2 dB) and ultra-broad integrated effective bandwidth (3.2–18.0 GHz), which were superior to many graphene-based composites, even those with high-density magnetic components. Carbon/carbon composites are new MAMs emerging in recent years, and thus the related reports are not as many as other kinds of composites. Although they display the potential to replace some magnetic MAMs, their RL characteristics including EABs are still far behind those we expected (Table 5).

### Ternary carbon-based dielectric composites

Inspired by the fact that the coordination mechanism of carbon materials and other dielectric components can also work for the consumption of EM energy effectively, some researchers conceived a new idea to upgrade the performance of carbon-based dielectric system by involving more dielectric components



**Table 5** Microwave absorption performance of carbon/carbon composites

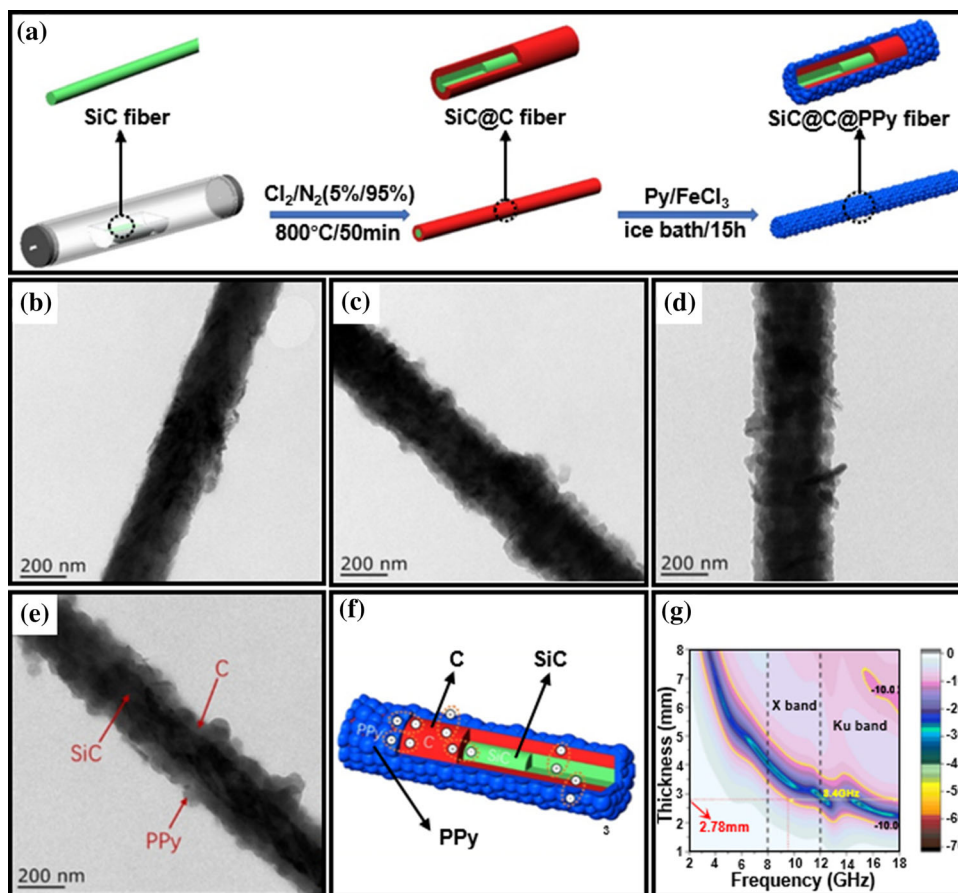
Absorber	Minimum RL (frequency, thickness)	EAB at 2.0 mm (range)	Reference
CNT@CF	– 42.0 dB (11.4 GHz, 2.5 mm)	Unshown	[171]
CNF-CNT	– 44.5 dB (10.7 GHz, 2.0 mm)	5.1 GHz (8.8–13.9 GHz)	[172]
Carbon black/RGO	– 47.5 dB (13.5 GHz, 2.2 mm)	1.4 GHz (13.0–14.4 GHz)	[174]
CNFs/RGO	– 38.1 dB (3.9 GHz, 5.0 mm)	2.2 GHz (12.0–14.2 GHz)	[175]
MWCNT/graphene foam	– 39.5 dB (11.6 GHz, 10.0 mm)	Unshown	[177]
Amorphous/nanocrystalline carbonized hydrochars	– 40.4 dB (10.2 GHz, 1.9 mm)	1.9 GHz (9.1–11.0 GHz)	[178]
Carbon microsphere@CNT	– 34.6 dB (8.8 GHz, 3.2 mm)	–	[179]
RGO/carbon microspheres/RGO	– 21.5 dB (18.0 GHz, 1.2 mm)	2.9 GHz (8.7–11.6 GHz)	[180]
RGO@carbon nanopolyhedrons	– 66.2 dB (6.2 GHz, 2.9 mm)	2.5 GHz (10.0–12.5 GHz)	[181]
Yolk-shell C@C microspheres	– 39.4 dB (16.5 GHz, 1.9 mm)	5.4 GHz (12.6–18.0 GHz)	[182]

[183, 184]. For instance, Chen et al. ever fabricated a series of brain fold-like polydopamine-modified PANI/nanodiamond (PANI/ND/PDA) ternary hybrids. They found that good dispersion of ND could induce low-frequency exchange resonance and domain wall resonance due to the nanoscaled EM effect, and  $\pi$ - $\pi$  interaction between PANI and PDA would contribute to carrier transportation, which enhanced low-frequency conductive loss and high-frequency eddy current loss [185]. However, in most cases, the construction of ternary dielectric composites was typically based on 1D CNTs or 2D RGO. A popular strategy was firstly to decorate CNTs or RGO with some inorganic nanoparticles, such as metal oxides and metal sulfides, and then to coat these intermediate binary composites with carbon or conductive polymer layer [186, 187]. As expected, the resultant ternary carbon-based composites will promise more or less enhancement in microwave absorption as compared with those binary ones. Hu et al. further directed the growth of  $K-\alpha$ MnO<sub>2</sub> on the surface of MoS<sub>2</sub>/RGO through hydrothermal KMnO<sub>4</sub> decomposition and demonstrated that  $K-\alpha$ MnO<sub>2</sub> could modulate the balance between relative complex permittivity and complex permeability like carbon layer and conductive polymer layer. Thanks to good impedance matching and attenuation capability, the RL values of RGO/MoS<sub>2</sub>/ $K-\alpha$ MnO<sub>2</sub> composites exceeding – 20 dB were achieved in a broad frequency range of 2.5–18.0 GHz [188]. To simplify the preparative process, Wu et al. developed a one-pot hydrothermal synthesis of ternary RGO/MWCNTs/CeO<sub>2</sub> composites as MAMs [189], while this process was too simple to guarantee homogeneous

distribution of various components, and the serious agglomeration, especially for CeO<sub>2</sub> nanoparticles, could be easily observed.

More recently, several groups have carried out elaborate microstructure design on these ternary carbon-based dielectric composites [190–192]. For example, Xu et al. obtained core-shell SiC@C nanowires by in situ etching SiC nanowires at high temperature under a mixed Cl<sub>2</sub>/N<sub>2</sub> atmosphere, and then conducted the polymerization of pyrrole monomers on the surface of SiC@C nanowires to produce dual-interfacial SiC@C@PPy nanofibers (Fig. 10a) [193]. It was clear that both carbon layer and PPy layer were successively and closely attached on the surface of SiC nanowires, and more importantly, the thickness of PPy layer could be finely regulated by the dosage of pyrrole monomers (Fig. 10b–e). EM tests revealed that there would be quite different charge distribution at various phase boundaries of SiC@C@PPy, which could result in the formation of dipole electric fields at these heterogeneous boundaries to promote the consumption of EM energy (Fig. 10f). When the mass ratio of SiC to pyrrole monomer reached 1:4, the final product would display excellent microwave absorption performance (Fig. 10g), including strong RL (– 59.3 dB) and broad effective bandwidth (8.4 GHz). Wang et al. designed hierarchical carbon fiber@MXene@MoS<sub>2</sub> with a similar dual core-shell microstructure, where MXene nanosheets were horizontally deposited on the surface of cetyltrimethylammonium bromide (CTAB)-modified CFs and then the vertical growth of MoS<sub>2</sub> nanosheets was realized through a hydrothermal reaction (Fig. 11a–f) [194]. In addition to dual interfacial polarization, other loss

**Figure 10** Synthetic process diagram of SiC@C@PPy nanofibers (a). TEM images of SiC@C@PPy-1 (b), SiC@C@PPy-2 (c), SiC@C@PPy-3 (d), and SiC@C@PPy-4 (e). Schematic illustration of dual-interfacial polarization effect (f). RL map of SiC@C@PPy-4 (15 wt%) (g). Adapted from Ref. [193], Copyright: 2020 American Chemical Society. Used with permission.



mechanisms, such as induced current, dipolar polarization, and multiple reflection and scattering were also confirmed to be contributed to microwave absorption (Fig. 11g). As a result, such hierarchical CF@MXene@MoS<sub>2</sub> had better RL characteristics than some conventional binary carbon-based dielectric composites (Fig. 11h). Thanks to diverse compositions, strong synergistic effects, and rich absorption mechanisms, these ternary carbon-based dielectric composites show some advantages in microwave absorption properties as compared with carbides/carbon and carbon/carbon composites (Table 6). However, the complex preparation and poor chemical homogeneity limit their development to some extent. The rational arrangement of different components in a simple way is highly desirable to further enhance the performance of these composites.

## Conclusions and outlooks

This review summarizes the recent developments of various carbon-based dielectric composites as promising microwave absorbing materials (MAMs). Those examples indicate that carbon-based dielectric system can not only produce comparable microwave absorption performance to conventional magnetic materials, but also untangle some intrinsic drawbacks of magnetic materials. Their excellent microwave absorption performance can be attributed to the following aspects: (1) the combination of carbon substrate and secondary dielectric components can create obvious complementary behaviors of their intrinsic properties, to optimize impedance matching; (2) the sufficient heterogeneous interfaces between different components can effectively induce strong interfacial polarization; (3) the multicomponent integration is conducive to the formation of conductive network, thus promoting the migration and hopping of electrons and reinforcing conductivity loss; (4) the elaborate microstructure design can supply more propagation paths for incident electromagnetic (EM)

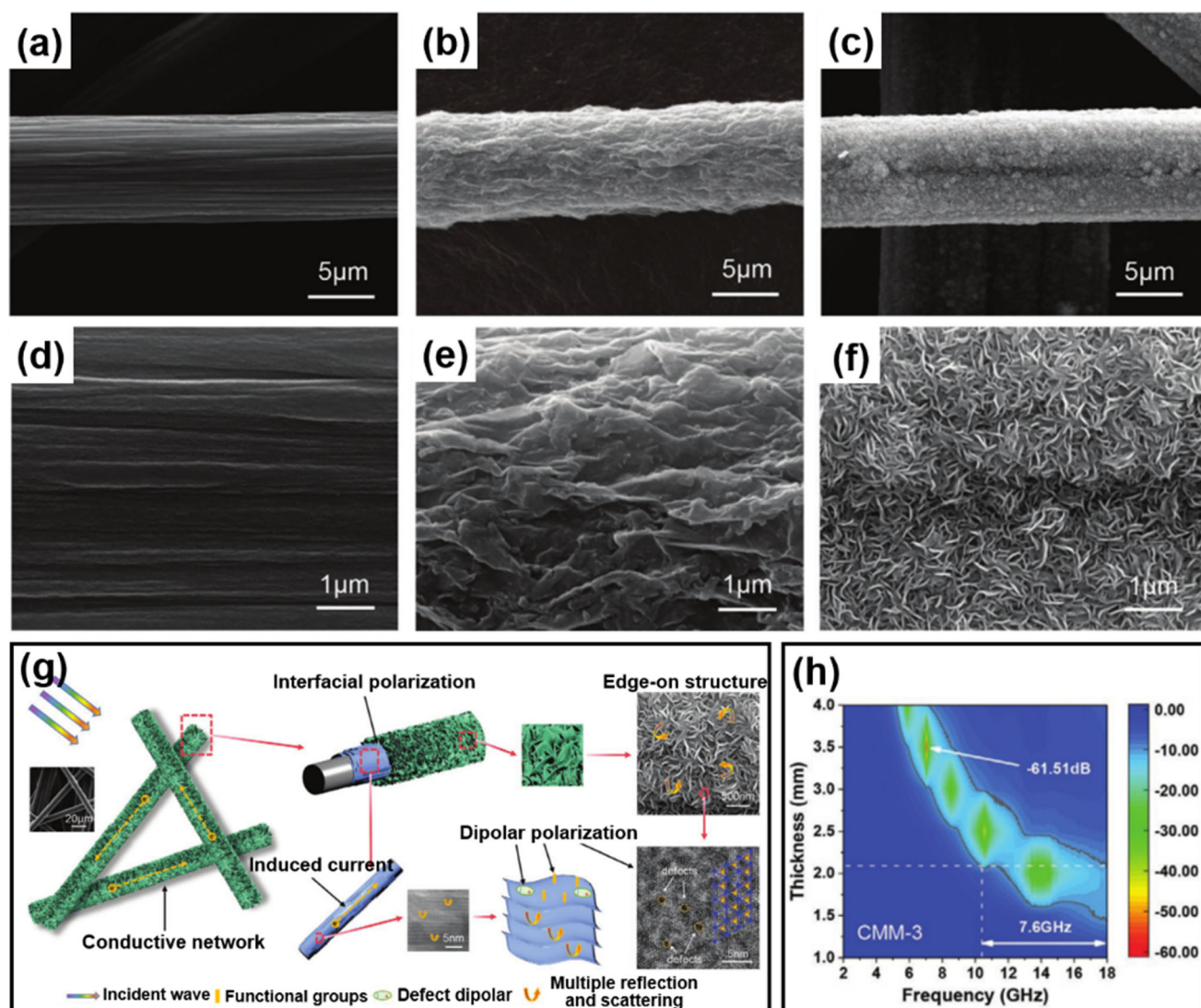


**Figure 11** SEM images of CF-CTAB (a and d), CF@MXene (b and e), and CF@MXene@MoS<sub>2</sub> (c and f). Schematic illustration of microwave absorption mechanisms (g) and RL map (h) of CF@MXene@MoS<sub>2</sub>. Adapted from Ref. [194], Copyright: 2020 Wiley. Used with permission.

**Table 6** Microwave absorption performance of ternary carbon-based dielectric composites

Absorber	Minimum RL (frequency, thickness)	EAB at 2.0 mm (range)	Reference
PANI/ND/PDA	– 24.3 dB (5.0 GHz, 5.6 mm) – 23.5 dB (15.9 GHz, 5.6 mm)	–	[185]
NiS <sub>2</sub> @RGO/PPy	– 58.7 dB (16.4 GHz, 2.0 mm)	4.3 GHz (13.7–18.0 GHz)	[187]
RGO/MoS <sub>2</sub> /K- $\alpha$ MnO <sub>2</sub>	– 71.7 dB (13.2 GHz, 3.8 mm)	Unshown	[188]
RGO/MWCNTs/CeO <sub>2</sub>	– 59.3 dB (4.6 GHz, 4.5 mm)	2.6 GHz (10.3–12.9 GHz)	[189]
CNT/RGO/ZIF-8	– 39.2 dB (6.5 GHz, 4.5 mm)	6.3 GHz (11.7–18.0 GHz)	[191]
SiC@C@PPy	– 59.3 dB (11.7 GHz, 3.0 mm)	2.0 GHz (16.0–18.0 GHz)	[193]
CF@MXene@MoS <sub>2</sub>	– 61.5 dB (7.0 GHz, 3.5 mm)	6.1 GHz (11.9–18.0 GHz)	[194]
Carbon cloths@C/CoS <sub>2</sub>	– 59.6 dB (9.2 GHz, 2.8 mm)	6.6 GHz (11.4–18.0 GHz)	[195]

**Table 7** The integrated EABs, preparation methods, advantages, and disadvantages of some representative carbon-based dielectric composites from different categories

Category	Sample	EAB with the integrating thickness of 1.0–5.0 mm	Preparation	Advantage	Disadvantage	Reference
Metal oxides/carbon composites	ZrO <sub>2</sub> /C	14.6 GHz (3.4–18.0 GHz)	MOF-derived method	Easy preparation, composition diversity, designable defects	Low conductive loss, poor acid resistance, easy agglomeration of metal oxides nanoparticles	[58]
	MnO@CNWs	14.0 GHz (4.0–18.0 GHz)	Hydrothermal method, calcination, etching			[62]
Metal sulfides/carbon composites	MoS <sub>2</sub> @hollow carbon spheres	14.5 GHz (3.2–17.7 GHz)	Template-etching-hydrothermal strategy	Easy preparation, composition diversity, in situ growth on carbon surface	Environmental toxicity, poor oxidation resistance, poor acid resistance	[27]
	MHSs-RGO	14.7 GHz (3.3–18.0 GHz)	One-pot template-free solvothermal method			[83]
Conductive polymers/carbon composites	MCNTs@PPy	12.8 GHz (5.2–18.0 GHz)	Carboxylation, in situ polymerization	Mild preparation, good conductivity, in situ polymerization on carbon surface	Natural degradation in conductivity, poor humidity resistance	[120]
	PPy/RGO	14.7 GHz (3.3–18.0 GHz)	Self-assembly method, chemical reduction			[130]
Carbides/carbon composites	SiC/C foam	12.4 GHz (5.6–18.0 GHz)	Pyrolysis, chemical vapor deposition	Thermal stability, good oxidation resistance, good acid resistance, durable performance	Low conductive loss, large particle size, high preparation temperature, poor chemical homogeneity	[144]
	Mo <sub>2</sub> C/C	14.5 GHz (3.5–18.0 GHz)	Solvothermal method, high-temperature pyrolysis, acidic etching			[166]
Carbon/carbon composites	RGO@carbon nanopolyhedrons	14.8 GHz (3.2–18.0 GHz)	In situ pyrolysis, acidic etching	Tunable dielectric property, good acid resistance, designable microstructure, durable performance	Complex preparation, poor chemical homogeneity, high preparation temperature	[181]
	Yolk-shell C@C microspheres	13.2 GHz (4.8–18.0 GHz)	Coating-coating-etching method			[182]
Ternary carbon-based dielectric composites	RGO/MoS <sub>2</sub> /K- $\alpha$ MnO <sub>2</sub>	15.5 GHz (2.5–18.0 GHz)	Modified Hummers' method, hydrothermal method	Composition diversity, strong synergistic effect, rich absorption mechanisms	Complex preparation, poor chemical homogeneity	[188]
	RGO/MWCNTs/CeO <sub>2</sub>	13.8 GHz (4.2–18.0 GHz)	Carboxylation, hydrothermal method			[189]



waves and stimulate multiple reflection and scattering to further consume EM energy.

Although substantial achievements have been made in carbon-based dielectric system, there still remain many challenges in this field. In order to clarify the related issues, we further compare microwave absorption properties, preparation methods, advantages, and disadvantages of some representative individuals from the categories mentioned above (Table 7). The integrated effective absorption bandwidth (EAB) from the absorber thickness of 1.0–5.0 mm is employed as an indicator to illustrate their universalities in different frequency ranges. As mentioned above, microwave absorption properties of various kinds of composites may be more or less different with a specific absorber thickness, while none of them can produce far superior microwave absorption performance to others yet, and meanwhile, they are also troubled by one problem or another. Based on this situation, some meaningful and promising breakthroughs are sum up as follows. First, the as-reported carbon-based dielectric composites are usually composed of no more than three dielectric components, and thus some pluralistic composites with more dielectric components should be developed. However, it is necessary to conduct a detailed study on the EM loss characteristics of each component and combine them in a reasonable way instead of blindly preparing multicomponent composites. Second, some defects, such as heteroatoms, atom vacancies, and grain boundaries, have demonstrated their positive effects on conductivity loss and polarization loss, while the structure–activity relationship between defect sites and microwave absorption performance is still unclear, which means that the defect engineering in MAMs will be established as early as possible to guide the fabrication of high-performance carbon-based dielectric composites. Third, it is found that most MAMs are mainly effective in the frequency range of 8.0–18.0 GHz, which seriously hinders their practical application in the field of electronics industry since the effective working frequency of many electronic devices is lower than 8.0 GHz. Rational construction of multicomponent composites with well-designed microstructures (e.g., hollow, multilayer, and small particle size) may induce the reflection and scattering behaviors of EM waves and intensify low-frequency attenuation capabilities (e.g., low-frequency exchange resonance and domain wall resonance, low-

frequency conductive loss), which is expected to break through the problem of low-frequency absorption. Fourth, the preparation method especially for multicomponent composites is usually complicated, which undoubtedly increases the difficulty of preparation and large-scale production, which undoubtedly increases the difficulty of preparation and large-scale production. In order to meet the requirements of practical application, it is of great significance to simplify the synthetic route. An attempt can be made to synthesize ordered microstructure by the means of self-assembly, and this will be a promising and challenging task to fabricate desirable multicomponent carbon-based dielectric composites. Fifth, some carbon-based dielectric composites are incapable of being applied in harsh conditions, e.g. strong acidity, high humidity, and concentrated salt mist. Some encapsulation and surface modifications are also in demand to improve their environmental tolerance. In summary, novel carbon-based dielectric system with reasonable compositions and elaborate microstructures will exhibit a bright prospect as high-performance MAMs against EM pollution.

## Acknowledgements

This work is supported by the financial support from Natural Science Foundation of China (21676065 and 21776053).

## Declarations

**Conflict of interest** The authors declare that there is no conflict of interest.

## References

- [1] Longair M (2015) ‘...a paper ...I hold to be great guns’: a commentary on Maxwell (1865) ‘A dynamical theory of the electromagnetic field’. *Phil Trans R Soc A* 373:20140473
- [2] Shahzad F, Alhabeab M, Hatter CB, Anasori B, Hong SM, Koo CM, Gogotsi Y (2016) Electromagnetic interference shielding with 2D transition metal carbides (MXenes). *Science* 353:1137–1140
- [3] Lv HL, Yang ZH, Wang PL, Ji GB, Song JZ, Zheng LR, Zeng HB, Xu ZJ (2018) A voltage-boosting strategy enabling a low-frequency, flexible electromagnetic wave absorption device. *Adv Mater* 30:1706343

- [4] Li Y, Liu XF, Nie XY, Yang WW, Wang YD, Yu RH, Shui JL (2019) Multifunctional organic-inorganic hybrid aerogel for self-cleaning, heat-insulating, and highly efficient microwave absorbing material. *Adv Funct Mater* 29:1807624
- [5] Ji H, Zhao R, Zhang N, Jin CX, Lu XF, Wang C (2018) Lightweight and flexible electrospun polymer nanofiber/metal nanoparticle hybrid membrane for high-performance electromagnetic interference shielding. *NPG Asia Mater* 10:749–760
- [6] Green M, Tian LH, Xiang P, Murowchick J, Tan XY, Chen XB (2018) Co<sub>2</sub>P nanoparticles for microwave absorption. *Mater Today Nano* 1:1–7
- [7] Zhang Y, Yang ZH, Li M, Yang LJ, Liu JC, Ha Y, Wu RB (2020) Heterostructured CoFe@C@MnO<sub>2</sub> nanocubes for efficient microwave absorption. *Chem Eng J* 382:123039
- [8] Green M, Liu ZQ, Xiang P, Liu Y, Zhou MJ, Tan XY, Huang FQ, Liu L, Chen XB (2018) Doped, conductive SiO<sub>2</sub> nanoparticles for large microwave absorption. *Light Sci Appl* 7:87
- [9] Tian LH, Yan XD, Xu JL, Wallenmeyer P, Murowchick J, Liu L, Chen XB (2015) Effect of hydrogenation on the microwave absorption properties of BaTiO<sub>3</sub> nanoparticles. *J Mater Chem A* 3:12550–12556
- [10] Green M, Tian LH, Xiang P, Murowchick J, Tan XY, Chen XB (2018) FeP nanoparticles: a new material for microwave absorption. *Mater Chem Front* 2:1119–1125
- [11] Liu Y, Fu YW, Liu L, Li W, Guan JG, Tong GX (2018) Low-cost carbothermal reduction preparation of monodisperse Fe<sub>3</sub>O<sub>4</sub>/C core-shell nanosheets for improved microwave absorption. *ACS Appl Mater Interfaces* 10:16511–16520
- [12] Liu DW, Du YC, Li ZN, Wang YH, Xu P, Zhao HH, Wang FY, Li CL, Han XJ (2018) Facile synthesis of 3D flower-like Ni microspheres with enhanced microwave absorption properties. *J Mater Chem C* 6:9615–9623
- [13] Qiu X, Wang LX, Zhu HL, Guan YK, Zhang QT (2017) Lightweight and efficient microwave absorbing materials based on walnut shell-derived nano-porous carbon. *Nanoscale* 9:7408–7418
- [14] Li XP, Deng ZM, Li Y, Zhang HB, Zhao S, Zhang Y, Wu XY, Yu ZZ (2019) Controllable synthesis of hollow microspheres with Fe@Carbon dual-shells for broad bandwidth microwave absorption. *Carbon* 147:172–181
- [15] Yang ZH, Zhang Y, Li M, Yang LJ, Liu JC, Hou Y, Yang Y (2019) Surface architecture of Ni-based metal organic framework hollow spheres for adjustable microwave absorption. *ACS Appl Nano Mater* 2:7888–7897
- [16] Wang X, Pan F, Xiang Z, Zeng QW, Pei K, Che RC, Lu W (2020) Magnetic vortex core-shell Fe<sub>3</sub>O<sub>4</sub>@C nanorings with enhanced microwave absorption performance. *Carbon* 157:130–139
- [17] Zhang WL, Zhang JM, Wu P, Chai GZ, Huang R, Ma F, Xu FF, Cheng HW, Chen YH, Ni X, Qiao L, Duan JL (2020) Parallel aligned nickel nanocone arrays for multi-band microwave absorption. *ACS Appl Mater Interfaces* 12:23340–23346
- [18] Wang FY, Wang N, Han XJ, Liu DW, Wang YH, Cui LR, Xu P, Du YC (2019) Core-shell FeCo@carbon nanoparticles encapsulated in polydopamine-derived carbon nanocages for efficient microwave absorption. *Carbon* 145:701–711
- [19] Kumar S, Arti KP, Singh N, Verma V (2019) Steady microwave absorption behavior of two-dimensional metal carbide MXene and polyaniline composite in X-band. *J Magn Magn Mater* 488:165364
- [20] Cheng JB, Zhao HB, Cao M, Li ME, Zhang AN, Li SL, Wang YZ (2020) Banana leaflike C-doped MoS<sub>2</sub> aerogels toward excellent microwave absorption performance. *ACS Appl Mater Interfaces* 12:26301–26312
- [21] Liang XH, Zhang XM, Liu W, Tang DM, Zhang BS, Ji GB (2016) A simple hydrothermal process to grow MoS<sub>2</sub> nanosheets with excellent dielectric loss and microwave absorption performance. *J Mater Chem C* 4:6816–6821
- [22] Quan B, Shi WH, Ong SJH, Lu XC, Wang PL, Ji GB, Guo YF, Zheng LR, Xu ZCJ (2019) Defect engineering in two common types of dielectric materials for electromagnetic absorption applications. *Adv Funct Mater* 29:1901236
- [23] Li G, Xie TS, Yang SL, Jin JH, Jiang JM (2012) Microwave absorption enhancement of porous carbon fibers compared with carbon nanofibers. *J Phys Chem C* 116:9196–9201
- [24] Chen C, Xi JB, Zhou EZ, Peng L, Chen ZC, Gao C (2018) Porous graphene microflowers for high-performance microwave absorption. *Nano-micro Lett* 10:26
- [25] Zhang Z, Zhao HQ, Gu WH, Yang LJ, Zhang BS (2019) A biomass derived porous carbon for broadband and lightweight microwave absorption. *Sci Rep* 9:18617
- [26] Wang BB, Fu QG, Song Q, Yu ZJ, Riedel R (2020) In situ growth of B<sub>4</sub>C nanowires on activated carbon felt to improve microwave absorption performance. *Appl Phys Lett* 116:203101
- [27] Ning MQ, Man QK, Tan GG, Lei ZK, Li JB, Li RW (2020) Ultrathin MoS<sub>2</sub> nanosheets encapsulated in hollow carbon spheres: a case of a dielectric absorber with optimized impedance for efficient microwave absorption. *ACS Appl Mater Interfaces* 12:20785–20796
- [28] Green M, Liu Z, Smedley R, Nawaz H, Li X, Huang F, Chen XB (2018) Graphitic carbon nitride nanosheets for microwave absorption. *Mater Today Phys* 5:78–86

- [29] Lin HR, Green M, Xu LJ, Chen XB, Ma BW (2019) Microwave absorption of organic metal halide nanotubes. *Adv Mater Interfaces* 7:1901270
- [30] Green M, Liu Z, Xiang P, Tan X, Huang F, Liu L, Chen XB (2018) Ferric metal-organic framework for microwave absorption. *Mater Today Chem* 9:140–148
- [31] Wen B, Cao MS, Hou ZL, Song WL, Zhang L, Lu MM, Jin HB, Fang XY, Wang WZ, Yuan J (2013) Temperature dependent microwave attenuation behavior for carbon-nanotube/silica composites. *Carbon* 65:124–139
- [32] Liu DW, Du YC, Xu P, Liu N, Wang YH, Zhao HH, Cui LR, Han XJ (2019) Waxberry-like hierarchical Ni@C microspheres with high-performance microwave absorption. *J Mater Chem C* 7:5037–5046
- [33] Cao MS, Han C, Wang XX, Zhang M, Zhang YL, Shu JC, Yang HJ, Fang XY, Yuan J (2018) Graphene nanohybrids: excellent electromagnetic properties for the absorbing and shielding of electromagnetic waves. *J Mater Chem C* 6:4586–4602
- [34] Tian CH, Du YC, Xu P, Qiang R, Wang Y, Ding D, Xue JL, Ma J, Zhao HT, Han XJ (2015) Constructing uniform core-shell PPy@PANI composites with tunable shell thickness toward enhancement in microwave absorption. *ACS Appl Mater Interfaces* 7:20090–20099
- [35] Zhao HH, Xu XZ, Wang YH, Fan DG, Liu DW, Lin KF, Xu P, Han XJ, Du YC (2020) Heterogeneous interface induced the formation of hierarchically hollow carbon microcubes against electromagnetic pollution. *Small* 16:2003407
- [36] Ohlan A, Singh K, Chandra A, Dhawan SK (2010) Microwave absorption behavior of core-shell structured poly (3,4-ethylenedioxy thiophene)-barium ferrite nanocomposites. *ACS Appl Mater Interfaces* 2:927–933
- [37] Zhao B, Zhao WY, Shao G, Fan BB, Zhang R (2015) Morphology-control synthesis of a core-shell structured NiCu alloy with tunable electromagnetic-wave absorption capabilities. *ACS Appl Mater Interfaces* 7:12951–12960
- [38] He S, Lu C, Wang GS, Wang JW, Guo HY, Guo L (2014) Synthesis and growth mechanism of white-fungus-like nickel sulfide microspheres, and their application in polymer composites with enhanced microwave-absorption properties. *Chem Plus Chem* 79:569–576
- [39] Xu DW, Yang S, Chen P, Yu Q, Xiong XH, Wang J (2019) Synthesis of magnetic graphene aerogels for microwave absorption by in-situ pyrolysis. *Carbon* 146:301–312
- [40] Lv HL, Zhang HQ, Zhao J, Ji GB, Du YW (2016) Achieving excellent bandwidth absorption by a mirror growth process of magnetic porous polyhedron structures. *Nano Res* 9:1813–1822
- [41] Liu PJ, Ng VMH, Yao ZJ, Zhou JT, Lei YM, Yang ZH, Lv HL, Kong LB (2017) Facile synthesis and hierarchical assembly of flower-like NiO structures with enhanced dielectric and microwave absorption properties. *ACS Appl Mater Interfaces* 9:16404–16416
- [42] Green M, Chen XB (2019) Recent progress of nanomaterials for microwave absorption. *J Materiomics* 5:503–541
- [43] Zeng XJ, Cheng XY, Yu RH, Stucky GD (2020) Electromagnetic microwave absorption theory and recent achievements in microwave absorbers. *Carbon* 168:606–623
- [44] Rao CNR (1989) Transition metal oxides. *Annu Rev Phys Chem* 40:291–326
- [45] Green M, Van Tran AT, Smedley R, Roach A, Murowchick J, Chen XB (2019) Microwave absorption of magnesium/hydrogen-treated titanium dioxide nanoparticles. *Nano Mater Sci* 1:48–59
- [46] Green M, Xiang P, Liu ZQ, Murowchick J, Tan XY, Huang FQ, Chen XB (2019) Microwave absorption of aluminum/hydrogen treated titanium dioxide nanoparticles. *J Materiomics* 5:133–146
- [47] Wan J, Yao X, Gao X, Xiao X, Li TQ, Wu JB, Sun WM, Hu ZM, Yu HM, Huang L, Liu ML, Zhou J (2016) Microwave combustion for modification of transition metal oxides. *Adv Funct Mater* 26:7263–7270
- [48] Green M, Li Y, Peng ZH, Chen XB (2020) Dielectric, magnetic, and microwave absorption properties of poly-oxometalate-based materials. *J Magn Magn Mater* 497:165974
- [49] Xia T, Zhang C, Oyler NA, Chen XB (2014) Enhancing microwave absorption of TiO<sub>2</sub> nanocrystals via hydrogenation. *J Mater Res* 29:2198–2210
- [50] Xia T, Cao YH, Oyler NA, Murowchick J, Liu L, Chen XB (2015) Strong microwave absorption of hydrogenated wide bandgap semiconductor nanoparticles. *ACS Appl Mater Interfaces* 7:10407–10413
- [51] Yu WL, Li WW, Wu J, Sun J, Hu ZG, Chu JH (2011) Diversity of electronic transitions and photoluminescence properties in nanocrystalline Mn/Fe-doped tin dioxide semiconductor films: an effect from oxygen pressure. *J Appl Phys* 110:123502
- [52] Tian LH, Xu JL, Just M, Green M, Liu L, Chen XB (2017) Broad range energy absorption enabled by hydrogenated TiO<sub>2</sub> nanosheets: from optical to infrared and microwave. *J Mater Chem C* 5:4645–4653
- [53] Dong JY, Ullal R, Han J, Wei SH, Ouyang X, Dong JZ, Gao W (2015) Partially crystallized TiO<sub>2</sub> for microwave absorption. *J Mater Chem A* 3:5285–5288
- [54] Cai M, Shui AZ, Wang X, He C, Qian JJ, Du B (2020) A facile fabrication and high-performance electromagnetic



- microwave absorption of ZnO nanoparticles. *J Alloy Compd* 842:155638
- [55] Xia T, Zhang C, Oyler NA, Chen XB (2013) Hydrogenated TiO<sub>2</sub> nanocrystals: a novel microwave absorbing material. *Adv Mater* 25:6905–6910
- [56] He JZ, Zeng QC, Sun X, Shu JC, Wang XX, Cao MS (2019) Axial ZnO rods wrapped with reduced graphene oxide: Fabrication, microstructure and highly efficient microwave absorption. *Mater Lett* 241:14–17
- [57] Yuchang Q, Qinlong W, Fa L, Wancheng Z (2016) Temperature dependence of the electromagnetic properties of graphene nanosheet reinforced alumina ceramics in the X-band. *J Mater Chem C* 4:4853–4862
- [58] Zhang X, Qiao J, Liu C, Wang FL, Jiang YY, Cui P, Wang Q, Wang Z, Wu LL, Liu JR (2020) A MOF-derived ZrO<sub>2</sub>/C nanocomposite for efficient electromagnetic wave absorption. *Inorg Chem Front* 7:385–393
- [59] Wan GP, Yu L, Peng XG, Wang GZ, Huang XQ, Zhao HN, Qin Y (2015) Preparation and microwave absorption properties of uniform TiO<sub>2</sub>@C core-shell nanocrystals. *RSC Adv* 5:77443–77448
- [60] Dong S, Tang WK, Hu PT, Zhao XG, Zhang XH, Han JC, Hu P (2019) Achieving excellent electromagnetic wave absorption capabilities by construction of MnO nanorods on porous carbon composites derived from natural wood via a simple route. *ACS Sustainable Chem Eng* 7:11795–11805
- [61] Wu C, Chen ZF, Wang ML, Cao X, Zhang Y, Song P, Zhang TY, Ye XL, Yang Y, Gu WH, Zhou JD, Huang YZ (2020) Confining tiny MoO<sub>2</sub> clusters into reduced graphene oxide for highly efficient low frequency microwave absorption. *Small* 16:2001686
- [62] Duan YL, Xiao ZH, Yan XY, Gao ZF, Tang YS, Hou LQ, Li Q, Ning GQ, Li YF (2018) Enhanced electromagnetic microwave absorption property of peapod-like MnO@carbon nanowires. *ACS Appl Mater Interfaces* 10:40078–40087
- [63] Cui LR, Tian CH, Tang LL, Han XJ, Wang YH, Liu DW, Xu P, Li CL, Du YC (2019) Space-confined synthesis of core-shell BaTiO<sub>3</sub>@Carbon microspheres as a high-performance binary dielectric system for microwave absorption. *ACS Appl Mater Interfaces* 11:31182–31190
- [64] Mo ZC, Yang RL, Lu DW, Yang LL, Hu QM, Li HB, Zhu H, Tang ZK, Gui XC (2019) Lightweight, three-dimensional carbon nanotube@TiO<sub>2</sub> sponge with enhanced microwave absorption performance. *Carbon* 144:433–439
- [65] Yang S, Guo X, Chen P, Xu DW, Qiu HF, Zhu XY (2019) Two-step synthesis of self-assembled 3D graphene/shuttle-shaped zinc oxide (ZnO) nanocomposites for high-performance microwave absorption. *J Alloy Compd* 797:1310–1319
- [66] Hu PT, Dong S, Li XT, Chen JM, Zhang XH, Hu P, Zhang SS (2019) A low-cost strategy to synthesize MnO nanorods anchored on 3D biomass-derived carbon with superior microwave absorption properties. *J Mater Chem C* 7:9219–9228
- [67] Wu Y, Shu RW, Zhang JB, Sun RR, Chen YN, Yuan J (2019) Oxygen vacancy defects enhanced electromagnetic wave absorption properties of 3D net-like multi-walled carbon nanotubes/cerium oxide nanocomposites. *J Alloy Compd* 785:616–626
- [68] Luo HL, Xiong GY, Yang ZW, Li QP, Ma CY, Li DY, Wu XB, Wang ZR, Wan YZ (2014) Facile preparation and extraordinary microwave absorption properties of carbon fibers coated with nanostructured crystalline SnO<sub>2</sub>. *Mater Res Bull* 53:123–131
- [69] Wang L, Xing HL, Gao ST, Ji XL, Shen ZY (2017) Porous flower-like NiO@graphene composites with superior microwave absorption properties. *J Mater Chem C* 5:2005–2014
- [70] Hu J, Shen Y, Xu LH, Liu YD (2020) Facile preparation of flower-like MnO<sub>2</sub>/reduced graphene oxide (RGO) nanocomposite and investigation of its microwave absorption performance. *Chem Phys Lett* 739:136953
- [71] Gao X, Wang Y, Wang QG, Wu XM, Zhang WZ, Zong M, Zhang LJ (2019) Facile synthesis of a novel flower-like BiFeO<sub>3</sub> microspheres/graphene with superior electromagnetic wave absorption performances. *Ceram Int* 45:3325–3332
- [72] Gao SY, Wang Q, Lin Y, Yang HB, Wang L (2019) Flower-like Bi<sub>0.9</sub>La<sub>0.1</sub>FeO<sub>3</sub> microspheres modified by reduced graphene oxide as a thin and strong electromagnetic wave absorber. *J Alloy Compd* 781:723–733
- [73] Wu Y, Shu RW, Shan XM, Zhang JB, Shi JJ, Liu Y, Zheng MD (2020) Facile design of cubic-like cerium oxide nanoparticles decorated reduced graphene oxide with enhanced microwave absorption properties. *J Alloy Compd* 817:152766
- [74] Baek K, Lee SY, Doh SG, Kim M, Hyun JK (2018) Axial oxygen vacancy-regulated microwave absorption in micron-sized tetragonal BaTiO<sub>3</sub> particles. *J Mater Chem C* 6:9749–9755
- [75] Jia ZR, Gao ZG, Kou KC, Feng AL, Zhang CH, Xu BH, Wu GL (2020) Facile synthesis of hierarchical A-site cation deficiency perovskite La<sub>x</sub>FeO<sub>3-y</sub>/RGO for high efficiency microwave absorption. *Compos Commun* 20:100344
- [76] Liu Y, Wu YX, Li KX, Wang J, Zhang CL, Ji JL, Wang WJ (2019) Amorphous SnS nanosheets/graphene oxide hybrid with efficient dielectric loss to improve the high-frequency

- electromagnetic wave absorption properties. *Appl Surf Sci* 486:344–353
- [77] Zhang J, Huang GZ, Zeng JH, Jiang XD, Shi YX, Lin SJ, Chen X, Wang HB, Kong Z, Xi JH, Ji ZG (2019) SnS<sub>2</sub> nanosheets coupled with 2D ultrathin MoS<sub>2</sub> nanolayers as face-to-face 2D/2D heterojunction photocatalysts with excellent photocatalytic and photoelectrochemical activities. *J Alloy Compd* 775:726–735
- [78] Tao F, Green M, Tran ATV, Zhang YL, Yin YS, Chen XB (2019) Plasmonic Cu<sub>9</sub>S<sub>5</sub> nanonets for microwave absorption. *ACS Appl Nano Mater* 2:3836–3847
- [79] Lu MM, Wang XX, Cao WQ, Yuan J, Cao MS (2016) Carbon nanotube-CdS core-shell nanowires with tunable and high-efficiency microwave absorption at elevated temperature. *Nanotechnology* 27:065702
- [80] Huang TY, He M, Zhou YM, Pan WL, Li SW, Ding BB, Huang S, Tong Y (2017) Fabrication and microwave absorption of multiwalled carbon nanotubes anchored with CoS nanoplates. *J Mater Sci* 28:7622–7632
- [81] Zhao B, Shao G, Fan BB, Zhao WY, Xie YJ, Zhang R (2015) Synthesis of flower-like CuS hollow microspheres based on nanoflakes self-assembly and their microwave absorption properties. *J Mater Chem A* 3:10345–10352
- [82] Zhang XJ, Li S, Wang SW, Yin ZJ, Zhu JQ, Guo AP, Wang GS, Yin PG, Guo L (2016) Self-supported construction of three-dimensional MoS<sub>2</sub> hierarchical nanospheres with tunable high-performance microwave absorption in broadband. *J Phys Chem C* 120:22019–22027
- [83] Chen DZ, Quan HY, Wang GS, Guo L (2013) Hollow  $\alpha$ -MnS spheres and their hybrids with reduced graphene oxide: synthesis, microwave absorption, and lithium storage properties. *ChemPlusChem* 78:843–851
- [84] Manzeli S, Ovchinnikov D, Pasquier D, Yazyev OV, Kis A (2017) 2D transition metal dichalcogenides. *Nat Rev Mater* 2:17033
- [85] Wang XX, Zhang WL, Ji XQ, Zhang BQ, Yu MX, Zhang W, Liu JQ (2016) 2D MoS<sub>2</sub>/graphene composites with excellent full Ku band microwave absorption. *RSC Adv* 6:106187–106193
- [86] Xu XS, Tian XJ, Sun BT, Liang ZQ, Cui HZ, Tian J, Shao MH (2020) 1T-phase molybdenum sulfide nanodots enable efficient electrocatalytic nitrogen fixation under ambient conditions. *Appl Catal B: Environ* 272:118984
- [87] Piao MX, Chu J, Wang X, Chi Y, Zhang H, Li CL, Shi HF, Joo MK (2018) Hydrothermal synthesis of stable metallic 1T phase WS<sub>2</sub> nanosheets for thermoelectric application. *Nanotechnology* 29:025705
- [88] Piao MX, Yang ZN, Liu F, Chu J, Wang X, Zhang H, Shi HF, Li CL (2020) Crystal phase control synthesis of metallic 1T-WS<sub>2</sub> nanosheets incorporating single walled carbon nanotubes to construct superior microwave absorber. *J Alloy Compd* 815:152335
- [89] Guo HQ, Wang L, You WB, Yang LT, Li X, Chen GY, Zheng Chen Wu, Qian X, Wang M, Che RC (2020) Engineering phase transformation of MoS<sub>2</sub>/RGO by N-doping as an excellent microwave absorber. *ACS Appl Mater Interfaces* 12:16831–16840
- [90] Tan HJ, Fan YM, Rong Y, Porter B, Lau CS, Zhou YQ, He ZY, Wang SS, Bhaskaran H, Warner JH (2016) Doping graphene transistors using vertical stacked monolayer WS<sub>2</sub> heterostructures grown by chemical vapor deposition. *ACS Appl Mater Interfaces* 8:1644–1652
- [91] Zhang ZY, Li WY, Yuen MF, Ng TW, Tang YB, Lee CS, Chen XF, Zhang WJ (2015) Hierarchical composite structure of few-layers MoS<sub>2</sub> nanosheets supported by vertical graphene on carbon cloth for high-performance hydrogen evolution reaction. *Nano Energy* 18:196–204
- [92] Zhang DQ, Wang HH, Cheng JY, Han CY, Yang XY, Xu JY, Shan GC, Zheng GP, Cao MS (2020) Conductive WS<sub>2</sub>-NS/CNTs hybrids based 3D ultra-thin mesh electromagnetic wave absorbers with excellent absorption performance. *Appl Surf Sci* 528:147052
- [93] Liu LL, Zhang S, Yan F, Li CY, Zhu CL, Zhang XT, Chen YJ (2018) Three-dimensional hierarchical MoS<sub>2</sub> nanosheets/ultralong N-doped carbon nanotubes as high-performance electromagnetic wave absorbing material. *ACS Appl Mater Interfaces* 10:14108–14115
- [94] Ning MQ, Kuang BY, Hou ZL, Wang L, Li JB, Zhao YJ, Jin HB (2019) Layer by layer 2D MoS<sub>2</sub>/rGO hybrids: an optimized microwave absorber for high-efficient microwave absorption. *Appl Surf Sci* 470:899–907
- [95] Xiao Y, Peng ZY, Zhang S, Jiang YH, Jing X, Yang XY, Zhang JM, Ni L (2019) Z-scheme CdIn<sub>2</sub>S<sub>4</sub>/BiOCl nanosheet face-to-face heterostructure: in-situ synthesis and enhanced interfacial charge transfer for high-efficient photocatalytic performance. *J Mater Sci* 54:9573–9590
- [96] Ye JJ, Qi L, Liu BB, Xu CX (2018) Facile preparation of hexagonal tin sulfide nanoplates anchored on graphene nanosheets for highly efficient sodium storage. *J Colloid Interface Sci* 513:188–197
- [97] Zhang DQ, Liu TT, Cheng JY, Cao Q, Zheng GP, Liang S, Wang H, Cao MS (2019) Lightweight and high-performance microwave absorber based on 2D WS<sub>2</sub>-RGO heterostructures. *Nano-Micro Lett* 11:38
- [98] Wang C, Mu CP, Xiang JY, Wang BC, Zhang C, Song JF, Wen FS (2018) Microwave synthesized In<sub>2</sub>S<sub>3</sub>@CNTs with excellent properties in lithium-ion battery and electromagnetic wave absorption. *Chin J Chem* 36:157–161
- [99] Wang YF, Chen DL, Yin X, Xu P, Wu F, He M (2015) Hybrid of MoS<sub>2</sub> and reduced graphene oxide: a lightweight

- and broadband electromagnetic wave absorber. *ACS Appl Mater Interfaces* 7:26226–26234
- [100] Liu C, Wang BC, Mu CP, Zhai K, Wen FS, Xiang JY, Nie AM, Liu ZY (2020) Enhanced microwave absorption properties of  $\text{MnS}_2$  microspheres interspersed with carbon nanotubes. *J Magn Magn Mater* 502:166432
- [101] Huang TY, He M, Zhou YM, Li SW, Ding BB, Pan WL, Huang S, Tong Y (2017) Solvothermal fabrication of CoS nanoparticles anchored on reduced graphene oxide for high-performance microwave absorption. *Synth Met* 224:46–55
- [102] Chai JX, Zhang DQ, Cheng JY, Jia YX, Ba XW, Gao Y, Zhu L, Wang H, Cao MS (2018) Facile synthesis of highly conductive  $\text{MoS}_2$ /graphene nanohybrids with hetero-structures as excellent microwave absorbers. *RSC Adv* 8:36616–36624
- [103] Pron A, Rannou P (2002) Processible conjugated polymers: from organic semiconductors to organic metals and superconductors. *Prog Polym Sci* 27:135–190
- [104] Koh YN, Mokhtar N, Phang SW (2018) Effect of microwave absorption study on polyaniline nanocomposites with untreated and treated double wall carbon nanotubes. *Polym Composite* 39:1283–1291
- [105] Green M, Tran ATV, Chen XB (2020) Maximizing the microwave absorption performance of polypyrrole by data-driven discovery. *Comp Sci Technol* 199:108332
- [106] Chandrasekhar P, Naishadham K (1999) Broadband microwave absorption and shielding properties of a poly (aniline). *Synth Met* 105:115–120
- [107] Green M, Tran ATV, Chen XB (2020) Obtaining strong, broadband microwave absorption of polyaniline through data-driven materials discovery. *Adv Mater Interfaces* 7:2000658
- [108] Green M, Tran ATV, Chen XB (2020) Realizing maximum microwave absorption of Poly (3,4-ethylenedioxythiophene) with a data-driven method. *ACS Appl Electron Mater* 2:2937–2944
- [109] Dong XL, Zhang XF, Huang H, Zuo F (2008) Enhanced microwave absorption in Ni/polyaniline nanocomposites by dual dielectric relaxations. *Appl Phys Lett* 92:013127
- [110] Sharma BK, Gupta AK, Khare N, Dhawan SK, Gupta HC (2009) Synthesis and characterization of polyaniline-ZnO composite and its dielectric behavior. *Synth Met* 159:391–395
- [111] Ma JL, Ren HD, Liu ZY, Zhou J, Wang YQ, Hu B, Liu Y, Kong LB, Zhang TS (2020) Embedded  $\text{MoS}_2$ -PANI nanocomposites with advanced microwave absorption performance. *Compos Sci Technol* 198:108239
- [112] Rahal M, Atassi Y, Ali NN, Alghoraibi I (2020) Novel microwave absorbers based on polypyrrole and carbon quantum dots. *Mater Chem Phys* 255:123491
- [113] Liu PB, Huang Y (2014) Decoration of reduced graphene oxide with polyaniline film and their enhanced microwave absorption properties. *J Polym Res* 21:430
- [114] Singh SK, Akhtar MJ, Kar KK (2020) Synthesis of a lightweight nanocomposite based on polyaniline 3D hollow spheres integrated milled carbon fibers for efficient X-band microwave absorption. *Ind Eng Chem Res* 59:9076–9084
- [115] Wu KH, Ting TH, Wang GP, Ho WD, Shih CC (2008) Effect of carbon black content on electrical and microwave absorbing properties of polyaniline/carbon black nanocomposites. *Polym Degrad Stabil* 93:483–488
- [116] Mahanta UJ, Gogoi JP, Borah D, Bhattacharyya NS (2019) Dielectric characterization and microwave absorption of expanded graphite integrated polyaniline multiphase nanocomposites in X-band. *IEEE T Dielect El In* 26:194–201
- [117] Qiu H, Wang J, Qi SH, He Z, Fan X, Dong YQ (2014) Microwave absorbing properties of multi-walled carbon nanotubes/polyaniline nanocomposites. *J Mater Sci* 26:564–570
- [118] Sharma BK, Khare N, Sharma R, Dhawan SK, Vankar VD, Gupta HC (2009) Dielectric behavior of polyaniline-CNTs composite in microwave region. *Compos Sci Technol* 69:1932–1935
- [119] Ting TH, Jau YN, Yu RP (2012) Microwave absorbing properties of polyaniline/multi-walled carbon nanotube composites with various polyaniline contents. *Appl Surf Sci* 258:3184–3190
- [120] Zhang K, Xie AM, Wu F, Jiang WC, Wang MY, Dong W (2016) Carboxyl multiwalled carbon nanotubes modified polypyrrole (PPy) aerogel for enhanced electromagnetic absorption. *Mater Res Express* 3:055008
- [121] Bai XX, Hu XJ, Zhou SY, Li LF, Rohwerder M (2015) Controllable synthesis of leaflet-like poly (3,4-ethylenedioxythiophene)/single-walled carbon nanotube composites with microwave absorbing property. *Compos Sci Technol* 110:166–175
- [122] Wang HG, Meng FB, Huang F, Jing CF, Li Y, Wei WW, Zhou ZW (2019) Interface modulating CNTs@PANi hybrids by controlled unzipping of the walls of CNTs to achieve tunable high-performance microwave absorption. *ACS Appl Mater Interfaces* 11:12142–12153
- [123] Cheng JY, Zhao B, Zheng SY, Yang JH, Zhang DQ, Cao MS (2015) Enhanced microwave absorption performance of polyaniline-coated CNT hybrids by plasma-induced graft polymerization. *Appl Phys A* 119:379–386



- [124] Buzaglo M, Bar IP, Varenik M, Shunak L, Pevzner S, Regev O (2017) Graphite-to-graphene: total conversion. *Adv Mater* 29:1603528
- [125] Duan YP, Liu J, Zhang YH, Wang TM (2016) First-principles calculations of graphene-based polyaniline nano-hybrids for insight of electromagnetic properties and electronic structures. *RSC Adv* 6:73915–73923
- [126] Yu HL, Wang TS, Wen B, Lu MM, Xu Z, Zhu CL, Chen YJ, Xue XY, Sun CW, Cao MS (2012) Graphene/polyaniline nanorod arrays: synthesis and excellent electromagnetic absorption properties. *J Mater Chem* 22:21679
- [127] Chen XN, Meng FC, Zhou ZW, Tian X, Shan LM, Zhu SB, Xu XL, Jiang M, Wang L, Hui D, Wang Y, Lu J, Gou JH (2014) One-step synthesis of graphene/polyaniline hybrids by in situ intercalation polymerization and their electromagnetic properties. *Nanoscale* 6:8140–8148
- [128] Liu J, Duan YP, Song LL, Zhang XF (2018) Constructing sandwich-like polyaniline/graphene oxide composites with tunable conjugation length toward enhanced microwave absorption. *Org Electron* 63:175–183
- [129] Zhang X, Huang Y, Liu PB (2016) Enhanced electromagnetic wave absorption properties of poly(3,4-ethylenedioxythiophene) nanofiber-decorated graphene sheets by non-covalent interactions. *Nano-Micro Lett* 8:131–136
- [130] Wang Y, Du YC, Wu B, Han BH, Dong SM, Han XJ, Xu P (2018) Fabrication of PPy nanosphere/rGO composites via a facile self-assembly strategy for durable microwave absorption. *Polymers* 10:998
- [131] Wu F, Wang Y, Wang MY (2014) Using organic solvent absorption as a self-assembly method to synthesize three-dimensional (3D) reduced graphene oxide (RGO)/poly(3,4-ethylenedioxythiophene) (PEDOT) architecture and its electromagnetic absorption properties. *RSC Adv* 4:49780–49782
- [132] Li X, Yu LM, Zhao WK, Shi YY, Yu LJ, Dong YB, Zhu YF, Fu YQ, Liu XD, Fu FY (2020) Prism-shaped hollow carbon decorated with polyaniline for microwave absorption. *Chem Eng J* 379:122393
- [133] Liu J, Wang ZZ, Rehman SU, Bi H (2017) Uniform core-shell PPy@carbon microsphere composites with a tunable shell thickness: the synthesis and their excellent microwave absorption performances in the X-band. *RSC Adv* 7:53104–53110
- [134] Chen XN, Chen JJ, Meng FB, Shan LM, Jiang M, Xu XL, Lu J, Wang Y, Zhou ZW (2016) Hierarchical composites of polypyrrole/graphene oxide synthesized by in situ intercalation polymerization for high efficiency and broadband responses of electromagnetic absorption. *Compos Sci Technol* 127:71–78
- [135] Wang Y, Wu XM, Zhang WZ (2016) Synthesis and high-performance microwave absorption of graphene foam/polyaniline nanorods. *Mater Lett* 165:71–74
- [136] Wang P, Cheng LF, Zhang YN, Yuan WY, Pan HX, Wu H (2018) Electrospinning of graphite/SiC hybrid nanowires with tunable dielectric and microwave absorption characteristics. *Compos Part A* 104:68–80
- [137] Dong S, Zhang WZ, Zhang XH, Hu P, Han JC (2018) Designable synthesis of core-shell SiCw@C heterostructures with thickness-dependent electromagnetic wave absorption between the whole X-band and Ku-band. *Chem Eng J* 354:767–776
- [138] Ma MD, Yang RL, Zhang C, Wang BC, Zhao ZS, Hu WT, Liu ZY, Yu DL, Wen FS, He JL, Tian YJ (2019) Direct large-scale fabrication of C-encapsulated B<sub>4</sub>C nanoparticles with tunable dielectric properties as excellent microwave absorbers. *Carbon* 148:504–511
- [139] Liu XX, Zhang ZY, Wu YP (2011) Absorption properties of carbon black/silicon carbide microwave absorbers. *Compos Part B: Eng* 42:326–329
- [140] Zhao JM, An WX, Li DA, Yang XL (2011) Synthesis and microwave absorption properties of SiC-carbon fibers composite in S and C band. *Synth Met* 161:2144–2148
- [141] Baskey HB, Singh SK, Akhtar MJ, Kar KK (2017) Investigation on the dielectric properties of exfoliated graphite-silicon carbide nanocomposites and their absorbing capability for the microwave radiation. *IEEE T Nanotechnol* 16:453–461
- [142] Xiao SS, Mei H, Han DY, Dassios KG, Cheng LF (2017) Ultralight lamellar amorphous carbon foam nanostructured by SiC nanowires for tunable electromagnetic wave absorption. *Carbon* 122:718–725
- [143] Li WC, Li CS, Lin LH, Wang Y, Zhang JS (2019) Foam structure to improve microwave absorption properties of silicon carbide/carbon material. *J Mater Sci Technol* 35:2658–2664
- [144] Ye XL, Chen ZF, Li M, Wang TM, Wu C, Zhang JX, Zhou QB, Liu HZ, Cui S (2019) Microstructure and microwave absorption performance variation of SiC/C foam at different elevated-temperature heat treatment. *ACS Sustainable Chem Eng* 7:18395–18404
- [145] Li BB, Mao BX, Wang XB, He T, Huang HQ (2020) Novel, hierarchical SiC nanowire-reinforced SiC/carbon foam composites: Lightweight, ultrathin, and highly efficient microwave absorbers. *J Alloy Compd* 829:154609
- [146] Yun T, Kim H, Iqbal A, Cho YS, Lee GS, Kim MK, Kim SJ, Kim D, Gogotsi Y, Kim SO, Koo CM (2020) Electromagnetic shielding of monolayer MXene assemblies. *Adv Mater* 32:1906769

- [147] Jhon YI, Koo J, Anasori B, Seo M, Lee JH, Gogotsi Y, Jhon YM (2017) Metallic MXene saturable absorber for femtosecond mode-locked lasers. *Adv Mater* 29:1702496
- [148] Sarycheva A, Gogotsi Y (2020) Raman spectroscopy analysis of the structure and surface chemistry of  $Ti_3C_2T_x$  MXene. *Chem Mater* 32:3480–3488
- [149] Cao MS, Cai YZ, He P, Shu JC, Cao WQ, Yuan J (2019) 2D MXenes: Electromagnetic property for microwave absorption and electromagnetic interference shielding. *Chem Eng J* 359:1265–1302
- [150] Iqbal A, Shahzad F, Hantanasirisakul K, Kim MK, Kwon J, Hong J, Kim H, Kim D, Gogotsi Y, Koo CM (2020) Anomalous absorption of electromagnetic waves by 2D transition metal carbonitride  $Ti_3CNT_x$  (MXene). *Science* 369:446–450
- [151] Qing YC, Nan HY, Luo F, Zhou WC (2017) Nitrogen-doped graphene and titanium carbide nanosheet synergistically reinforced epoxy composites as high-performance microwave absorbers. *RSC Adv* 7:27755–27761
- [152] Ma WL, Chen HH, Hou SY, Huang ZY, Huang Y, Xu ST, Fan F, Chen YS (2019) Compressible highly stable 3D porous MXene/GO foam with a tunable high-performance stealth property in the terahertz band. *ACS Appl Mater Interfaces* 11:25369–25377
- [153] Dai BZ, Zhao B, Xie X, Su TT, Fan BB, Zhang R, Yang R (2018) Novel two-dimensional  $Ti_3C_2T_x$  MXenes/nano-carbon sphere hybrids for high-performance microwave absorption. *J Mater Chem C* 6:5690–5697
- [154] Li XL, Yin XW, Han MK, Song CQ, Xu HL, Hou ZX, Zhang LT, Cheng LF (2017)  $Ti_3C_2$  MXenes modified with in situ grown carbon nanotubes for enhanced electromagnetic wave absorption properties. *J Mater Chem C* 5:4068–4074
- [155] Han MK, Yin XW, Li XL, Anasori B, Zhang LT, Cheng LF, Gogotsi Y (2017) Laminated and two-dimensional carbon-supported microwave absorbers derived from MXenes. *ACS Appl Mater Interfaces* 9:20038–20045
- [156] Li XL, Yin XW, Song CQ, Han MK, Xu HL, Duan WY, Cheng LF, Zhang LT (2018) Self-assembly core-shell graphene-bridged hollow MXenes spheres 3D foam with ultrahigh specific EM absorption performance. *Adv Funct Mater* 28:1803938
- [157] Li Y, Meng FB, Mei Y, Wang HG, Guo YF, Wang Y, Peng FX, Huang F, Zhou ZW (2020) Electrospun generation of  $Ti_3C_2T_x$  MXene@graphene oxide hybrid aerogel microspheres for tunable high-performance microwave absorption. *Chem Eng J* 391:123512
- [158] Wang LB, Liu H, Lv XL, Cui GZ, Gu GX (2020) Facile synthesis 3D porous MXene  $Ti_3C_2T_x$ @RGO composite aerogel with excellent dielectric loss and electromagnetic wave absorption. *J Alloy Comp* 828:154251
- [159] Zhan JM, Jian WR, Tang XC, Han YL, Li WH, Yao XH, Meng LY (2019) Tensile deformation of nanocrystalline Al-matrix composites: Effects of the SiC particle and graphene. *Comp Mater Sci* 156:187–194
- [160] Zou JP, Wang ZZ, Yan MQ, Bi H (2014) Enhanced interfacial polarization relaxation effect on microwave absorption properties of submicron-sized hollow  $Fe_3O_4$  hemispheres. *J Phys D: Appl Phys* 47:275001
- [161] Bokhonov B, Borisova Y, Korchagin M (2004) Formation of encapsulated molybdenum carbide particles by annealing mechanically activated mixtures of amorphous carbon with molybdenum. *Carbon* 42:2067–2071
- [162] Fan XJ, Liu YY, Peng ZW, Zhang ZH, Zhou HQ, Zhang XM, Yakobson BI, Goddard WA, Guo X, Hauge RH, Tour JM (2017) Atomic H-induced  $Mo_2C$  hybrid as an active and stable bifunctional electrocatalyst. *ACS Nano* 11:384–394
- [163] Li XP, Li ZQ, Que LK, Ma YJ, Zhu L, Pei CH (2020) Electromagnetic wave absorption performance of graphene/SiC nanowires based on graphene oxide. *J Alloy Compd* 835:155172
- [164] Wang YH, Han XJ, Xu P, Liu DW, Cui LR, Zhao HH, Du YC (2019) Synthesis of pomegranate-like  $Mo_2C@C$  nanospheres for highly efficient microwave absorption. *Chem Eng J* 372:312–320
- [165] Dai SS, Cheng Y, Quan B, Liang XH, Liu W, Yang ZH, Ji GB, Du YW (2018) Porous-carbon-based  $Mo_2C$  nanocomposites as excellent microwave absorber: A new exploration. *Nanoscale* 10:6945–6953
- [166] Wang YH, Li CL, Han XJ, Liu DW, Zhao HH, Li ZN, Xu P, Du YC (2018) Ultrasmall  $Mo_2C$  nanoparticle-decorated carbon polyhedrons for enhanced microwave Absorption. *ACS Appl Nano Mater* 1:5366–5376
- [167] Lian YL, Han BH, Liu DW, Wang YH, Zhao HH, Xu P, Han XJ, Du YC (2020) Solvent-free synthesis of ultrafine tungsten carbide nanoparticles-decorated carbon nanosheets for microwave absorption. *Nano-Micro Lett* 12:153
- [168] Behtash M, Nazir S, Wang YQ, Yang K (2016) Polarization effects on the interfacial conductivity in  $LaAlO_3/SrTiO_3$  heterostructures: a first-principles study. *Phys Chem Chem Phys* 18:6831–6838
- [169] Sun Y, Sun YG (2020) Precursor infiltration and pyrolysis cycle-dependent mechanical and microwave absorption performances of continuous carbon fibers-reinforced boron-containing phenolic resins for low-density carbon-carbon composites. *Ceram Int* 46:15167–15175
- [170] Xu HL, Yin XW, Zhu M, Li MH, Zhang H, Wei HJ, Zhang LT, Cheng LF (2019) Constructing hollow graphene nano-

- spheres confined in porous amorphous carbon particles for achieving full X band microwave absorption. *Carbon* 142:346–353
- [171] Singh SK, Akhtar MJ, Kar KK (2018) Hierarchical carbon nanotube-coated carbon fiber: ultra lightweight, thin, and highly efficient microwave absorber. *ACS Appl Mater Interfaces* 10:24816–24828
- [172] Zhang T, Xiao B, Zhou PY, Xia L, Wen GW, Zhang HB (2017) Porous-carbon-nanotube decorated carbon nanofibers with effective microwave absorption properties. *Nanotechnology* 28:355708
- [173] Zhao JG, Xing BY, Yang H, Pan QL, Li ZP, Liu ZJ (2016) Growth of carbon nanotubes on graphene by chemical vapor deposition. *New Carbon Mater* 31:31–36
- [174] Tang J, Bi S, Wang X, Hou GL, Su XJ, Liu CH, Lin YY, Li H (2019) Excellent microwave absorption of carbon black/reduced graphene oxide composite with low loading. *J Mater Sci* 54:13990–14001
- [175] Zhang XX, Wang J, Su XG, Huo SQ (2019) Facile synthesis of reduced graphene oxide-wrapped CNFs with controllable chemical reduction degree for enhanced microwave absorption performance. *J Colloid Interface Sci* 553:402–408
- [176] Lv HL, Li Y, Jia ZR, Wang LJ, Guo XQ, Zhao B, Zhang R (2020) Exceptionally porous three-dimensional architectural nanostructure derived from CNTs/graphene aerogel towards the ultra-wideband EM absorption. *Compos Part B* 196:108122
- [177] Chen HH, Huang ZY, Huang Y, Zhang Y, Ge Z, Qin B, Liu ZF, Shi Q, Xiao PS, Yang Y, Zhang TF, Chen YS (2017) Synergistically assembled MWCNT/graphene foam with highly efficient microwave absorption in both C and X bands. *Carbon* 124:506–514
- [178] Qi YJ, Wei DC, Shi GM, Zhang M, Qi Y (2019) Amorphous/nanocrystalline carbonized hydrochars with isomeric heterogeneous interfacial polarizations for high-performance microwave absorption. *Sci Rep* 9:12429
- [179] Li MH, Fan XM, Xu HL, Ye F, Xue JM, Li XQ, Cheng LF (2020) Controllable synthesis of mesoporous carbon hollow microspheres twined by CNT for enhanced microwave absorption performance. *J Mater Sci Technol* 59:164–172
- [180] Wang Y, Du YC, Qiang R, Tian CH, Xu P, Han XJ (2016) Interfacially engineered sandwich-like rGO/carbon microspheres/rGO composite as an efficient and durable microwave absorber. *Adv Mater Interfaces* 3:1500684
- [181] Zhao HH, Han XJ, Li ZN, Liu DW, Wang YH, Wang Y, Zhou W, Du YC (2018) Reduced graphene oxide decorated with carbon nanopolyhedrons as an efficient and lightweight microwave absorber. *J Colloid Interface Sci* 528:174–183
- [182] Qiang R, Du YC, Wang Y, Wang N, Tian CH, Ma J, Xu P, Han XJ (2016) Rational design of yolk-shell C@C microspheres for the effective enhancement in microwave absorption. *Carbon* 98:599–606
- [183] Zhao J, Lu YJ, Ye WL, Wang L, Liu B, Lv SS, Chen LX, Gu JW (2019) Enhanced wave-absorbing performances of silicone rubber composites by incorporating C-SnO<sub>2</sub>-MWCNT absorbent with ternary heterostructure. *Ceram Int* 45:20282–20289
- [184] Thi QV, Lim S, Jang E, Kim J, Van Khoi N, Tung NT, Sohn D (2020) Silica particles wrapped with poly(aniline-copyrrole) and reduced graphene oxide for advanced microwave absorption. *Mater Chem Phys* 244:122691
- [185] Chen XN, Zhou JX, Zhang Y, Zhu SB, Tian X, Meng FC, Cui LY, Xue PH, Huang RX, Sun JC (2019) Polydopamine-modified polyaniline/nanodiamond ternary hybrids with brain fold-like surface for enhanced dual band electromagnetic absorption. *ACS Appl Polym Mater* 1:405–413
- [186] Zhao J, Zhang JL, Wang L, Lyu SS, Ye WL, Xu BB, Qiu H, Chen LX, Gu JW (2020) Fabrication and investigation on ternary heterogeneous MWCNT@TiO<sub>2</sub>-C fillers and their silicone rubber wave-absorbing composites. *Compos Part A* 129:105714
- [187] Zhang Z, Lv Q, Chen YW, Yu HT, Liu H, Cui GZ, Sun XD, Li L (2019) NiS<sub>2</sub>@rGO nanosheet wrapped with PPy aerogel: a sandwich-like structured composite for excellent microwave absorption. *Nanomaterials* 9:833
- [188] Hu Q, Fang Y, Wang JJ, Du Z, Song QQ, Guo ZL, Huang Y, Lin J, Tang CC (2019) Novel hierarchical RGO/MoS<sub>2</sub>/K- $\alpha$ MnO<sub>2</sub> composite architectures with enhanced broadband microwave absorption performance. *J Mater Chem C* 7:13878–13886
- [189] Wu Y, Shu RW, Zhang JB, Wan ZL, Shi JJ, Liu Y, Zhao GM, Zheng MD (2020) Oxygen vacancies regulated microwave absorption properties of reduced graphene oxide/multi-walled carbon nanotubes/ cerium oxide ternary nanocomposite. *J Alloy Compd* 819:152944
- [190] Lai YY, Lv LZ, Fu HQ (2020) Preparation and study of Al<sub>2</sub>O<sub>3</sub>@PPy@rGO composites with microwave absorption properties. *J Alloy Compd* 832:152957
- [191] Wang JX, Yang JF, Yang J, Zhang H (2020) Design of novel CNT/RGO/ZIF-8 ternary hybrid structure for lightweight and highly effective microwave absorption. *Nanotechnology* 31:414001
- [192] Ren FY, Xue JM, Liu XL, Cheng LF (2020) In situ construction of CNWs/SiC-NWs hybrid network reinforced SiCN with excellent electromagnetic wave absorption properties in X band. *Carbon* 168:278–289
- [193] Xu C, Wu F, Duan LQ, Xiong ZM, Xia YL, Yang ZQ, Sun MX, Xie AM (2020) Dual-interfacial polarization



- enhancement to design tunable microwave absorption nanofibers of SiC@C@PPy. *ACS Appl Electron Mater* 2:1505–1513
- [194] Wang JQ, Liu L, Jiao SL, Ma KJ, Lv J, Yang JJ (2020) Hierarchical carbon fiber@MXene@MoS<sub>2</sub> core-sheath synergistic microstructure for tunable and efficient microwave absorption. *Adv Funct Mater* 30:2002595
- [195] Liu PB, Zhu CY, Gao S, Guan C, Huang Y, He WJ (2020) N-doped porous carbon nanoplates embedded with CoS<sub>2</sub> vertically anchored on carbon cloths for flexible and ultrahigh microwave absorption. *Carbon* 163:348–359

**Publisher's Note** Springer Nature remains neutral with regard to jurisdictional claims in published maps and institutional affiliations.